Received: 1 August 2025 | Revised: 10 November 2025 | Accepted: 21 November 2025 | Published online: 11 December 2025

RESEARCH ARTICLE

Journal of Computational and Cognitive Engineering
2025, Vol. XX(XX) 1–21
DOI: 10.47852/bonviewJCCE52027030

BON VIEW PUBLISHING

Beta-Transformed Inverse Length-Biased Exponential Distribution: Properties and Applications

Jabir Bengalath[1], Mohamed Nejib Ouertani[2,*], Hanene Hamdani[2], Fasna Kottakkunnan[3] and Mohammed Elgarhy[4,5]

[1] *Government Arts and Science College Calicut, University of Calicut, India*

[2] *College of Business, Imam Mohammad Ibn Saud Islamic University (IMSIU), Saudi Arabia*

[3] *Department of Statistics, Stockholm University, Sweden*

[4] *Department of Basic Sciences, Higher Institute of Administrative Sciences, Egypt*

[5] *Department of Computer Engineering, Biruni University, Türkiye*

Abstract: In this article, we introduce a novel probability distribution, the beta-transformed inverse length-biased exponential (BTILBE) distribution, derived from the exponential distribution using the beta transformation technique. This approach is advantageous because it introduces no additional parameters beyond those of the baseline distribution. The BTILBE distribution features a highly flexible hazard function and exhibits unique statistical properties that we comprehensively analyze. We explore key statistical characteristics, including moments, inverted moments, incomplete moments, generating functions, mean residual life, and mean inactivity times. Additionally, we provide numerical illustrations of moments, skewness, kurtosis, and the coefficient of variation to offer a thorough understanding of the proposed model. We also derive expressions for entropy measures, such as Shannon entropy, Tsallis entropy, and Rényi entropy, accompanied by numerical examples. The parameters of the BTILBE distribution are estimated using maximum likelihood estimation (MLE), and a simulation study validates their accuracy. To demonstrate the model's practical applicability, we apply it to two real-world datasets, where the BTILBE distribution exhibits exceptional flexibility and outperforms several established distributions, establishing it as a robust and valuable tool for statistical modeling.

Keywords: beta transformation, inverse length-biased exponential distribution, statistical properties, maximum likelihood estimation, simulation, applications

1. Introduction

Statistical distributions play a pivotal role in modeling and analyzing various types of data, making the development of new distributions a crucial aspect of statistical theory and practice. Over the years, numerous distributions have been introduced to model datasets across diverse fields, including environmental studies, ecology, medical research, and even COVID-19 data analysis. Among these, exponential distribution stands out as one of the most widely used continuous distributions, particularly for modeling the time elapsed between events. Its popularity has led to the development of numerous generalizations, such as the generalized exponential extended exponentiated family of distributions [1], extended exponential distribution [2], Weibull exponentiated-exponential (WEE) distribution [3], modified generalized linear exponential distribution [4], Modi inverse exponential distribution [5], unit logistic exponential distribution [6], neutrosophic logic Odd Lomax generalized exponential [7], odd reparameterized exponential family of distributions [8], statistical analysis of alpha-power exponential distribution using unified hybrid censored data [9], generalization Erlang truncated exponential distribution [10], log exponential-power distribution [11], discrete exponential generalized-G family of distributions [12], exponentiated generalized Weibull exponential distribution [13], exponentiated inverse exponential distribution [14], statistical inference of modified Kies exponential distribution under ranked set sampling [15], type II general inverse exponential family of distributions [16], half logistic modified Kies exponential distribution [17], a new exponential family of distributions [18], and extended exponential distribution [19]. For more details, see works by Noori et al. [20] and Hussain et al. [21].

Dara and Ahmad [22], following the initial work of Fisher [23] and Rao [24], formulated a novel exponential distribution extension, which they coined the moment-exponential distribution. It is also known as the length-biased exponential (LBE) distribution. The LBE distribution is especially useful for studying failure processes or lifetime data because it flexibly captures many real-world failure times or durations. This flexibility makes it a better fit for lifespan data than a simple exponential model. It also improves the accuracy of handling complex and various patterns in these data. The probability density function (PDF) and cumulative distribution function (CDF):

$$G(y,\theta) = 1 - \left(1 + \frac{y}{\theta}\right) e^{-\frac{y}{\theta}}, \quad \theta > 0, \tag{1}$$

$$f(y,\theta) = \frac{y}{\theta^2} e^{-\frac{y}{\theta}}, \quad \theta > 0, \tag{2}$$

where θ represents the scale parameter.

The shape of the PDF is highly influenced by the value of the shape parameter, with various values resulting in distinct shapes of the density curve. Over the years, researchers have proposed various extensions and generalizations of the LBE distribution to enhance its flexibility and applicability. Notable among these extensions are

***Corresponding author:** Mohamed Nejib Ouertani, College of Business, Imam Mohammad Ibn Saud Islamic University (IMSIU), Saudi Arabia. Email: mnouertani@imamu.edu.sa

the Marshall-Olkin LBE (MOLBE) distribution [25] and the Harris extended LBE distribution [26]. These extended distributions have further enriched the family of LBE distributions, offering more versatile tools for modeling and analyzing complex datasets.

The inverse LBE (ILBE) distribution [27] is constructed using the random variable $T = \frac{1}{X}$, where X follows the LBE distribution. The CDF of the ILBE distribution is described as:

$$F(x;\theta) = \left(1 + \frac{\theta}{x}\right) e^{-\frac{\theta}{x}}, \quad x \geq 0,\, \theta > 0. \tag{3}$$

$$g(x,\theta) = \frac{\theta^2}{x^3} e^{-\frac{\theta}{x}}, \quad x \geq 0,\, \theta > 0. \tag{4}$$

The application of order statistics moments is established in statistical literature and is applied in statistical modeling, inference, decision-making procedures, and nonparametric statistics. Several researchers have derived recurrence relations for individual and product moments of order statistics, either for a general form of distributions or for specific distributions. Some of the significant contributions in this direction are discussed in references [28–34] and others. These recurrence relations serve as the core of understanding the behavior of order statistics and their applications.

Moreover, moments of order statistics play a crucial role in deriving the best linear unbiased estimates (BLUEs) for the location and scale parameters of distributions, particularly in the context of complete and type-II censored samples. Their significance in statistical estimation and inference underscores their enduring value in both theoretical and applied statistics.

Recent developments in distribution theory have seen a growing interest among researchers in introducing innovative methods to expand the family of probability distributions. This expansion has been achieved through various approaches. In the statistical literature, numerous transformations have been proposed to generate new CDFs from existing ones. Among the most notable transformations are the power transformation [35], the quadratic rank transformation map (QRTM) [36], and the DUS transformation [37]. Additionally, Maurya et al. [38] proposed the GDUS transformation, a generalization of the DUS transformation. A trigonometric-based transformation called the PCM transformation was introduced by Kumar et al. [39], while Mahdavi and Kundu [40] introduced the alpha power transformation (APT). More recently, Lone and Jan [41] introduced a novel method called the Pi-exponentiated approach for constructing distributions. Additionally, Dileepkumar and Bengalath [42] developed a new parsimonious transformation called the DM transformation, utilizing a distortion function to generate new distributions. These advancements highlight the continuous evolution and diversification of techniques in the field of distribution theory. In the present study, we applied a novel transformation, proposed by Fasna [43], called the beta transformation for $x \in \mathbb{R}$, as described in the following:

$$G(x) = \begin{cases} \frac{\beta}{\beta-1}[1 - \beta^{-F(x)}] & \text{if } \beta > 0, \beta \neq 1 \\ F(x) & \text{if } \beta = 1 \end{cases}, \tag{5}$$

where $G(x)$ and $F(x)$ are the CDFs of the proposed transformation and the baseline distribution. By differentiating Equation (5) w.r.t. x, we get the pdf $g(x)$, which is given by:

$$g(x) = \begin{cases} \frac{\beta \log \beta}{\beta-1} f(x)\beta^{-F(x)} & \text{if } \beta > 0, \beta \neq 1 \\ f(x) & \text{if } \beta = 1 \end{cases}. \tag{6}$$

The development of the BTILBE distribution is driven by the need to address limitations in existing statistical models and to provide a versatile tool for modeling complex data across various domains. This research is motivated by the following key considerations:

1) **Introducing the new generalized version of inverse length-biased distribution:** This study proposes a new probability distribution by applying beta transformation to the inverse length-biased distribution, which serves as the baseline. The statistical properties of this new model are systematically explored, extending the capabilities of the baseline and offering a robust framework for addressing diverse data structures.
2) **Exceptional shape flexibility:** The BTILBE distribution exhibits exceptional shape flexibility, effectively modeling a wide range of data shapes, including right-skewed and symmetric distributions. It overcomes the limitations of traditional length-biased models, providing superior fits to complex datasets with comparable or fewer parameters, making it an efficient choice for real-world applications.
3) **Modeling heavy-tailed data:** As the parameters θ and β increase, the BTILBE distribution exhibits heavier tails, making it particularly well suited for datasets with extreme values. This characteristic is invaluable in fields such as financial risk modeling and survival analysis, where capturing outliers is crucial for accurate inference.
4) **Leveraging the beta distribution's versatility:** By harnessing the beta distribution's well-known ability to generate diverse shapes, the BTILBE distribution enhances the adaptability of the inverse length-biased baseline. This transformation enables the model to effectively capture complex, real-world patterns that simpler models struggle to represent.
5) **Superior fit and efficiency:** Empirical results demonstrate that the BTILBE distribution consistently outperforms competing models in goodness-of-fit metrics, even when those models use an equal or greater number of parameters. This efficiency makes it an attractive option for statistical modeling in resource-constrained environments.
6) **Driving innovation despite challenges:** While the incorporation of the beta transformation introduces complexity in parameter estimation (e.g., in maximum likelihood methods), it encourages the development of innovative computational strategies to ensure robust performance, thereby advancing statistical methodology.

This article is structured as follows: Section 2 introduces the PDF, CDF, survival function (SF), and hazard rate function (HRF) of the proposed distribution. Section 3 explores various statistical properties of the distribution, including moments, inverted moments, incomplete moments, and the moment generating function (MGF). In Section 4, key reliability characteristics of the distribution are examined. Section 5 delves into different entropy measures, such as Shannon entropy, Tsallis entropy, and Rényi entropy. Section 6 presents the estimation of unknown parameters using the maximum likelihood method. Section 8 demonstrates the practical application of the proposed model through the analysis of a real-world dataset. Finally, Section 9 provides the conclusion of the study.

2. Beta-Transformed Inverted Length-Biased Exponential Distribution

In this section, we develop a novel generalization of the inverse length-biased exponential (ILBE) distribution, referred to as the beta-transformed inverse length-biased (BTILBE) distribution . This generalization is based on the innovative method [43], which applied the beta transformation (BT) method to the exponential distribution and extensively studied the properties of the resulting beta-transformed exponential distribution. Fasna [44] applied the BT method to the Cauchy distribution and studied various properties of the beta-transformed

Cauchy distribution. Building on the BT method, we introduce a new three-parameter distribution, called the BTILBE. We derive its fundamental PDF and HRF and provide graphical representations to illustrate its behavior. In addition, CDF, SF, reversed HRF, and cumulative HRF are presented to offer a comprehensive characterization of BTILBE distribution. The CDF and PDF of the BTILBE distribution can be explicitly formulated by substituting Equations (3) and (4) into Equations (5) and (6), as detailed below.

$$G(x) = \begin{cases} \frac{\beta}{\beta-1}[1-\beta^{-(1+\frac{\theta}{x})e^{-\frac{\theta}{x}}}] & \text{if } \beta \neq 1 \\ (1+\frac{\theta}{x})e^{-\frac{\theta}{x}} & \text{if } \beta = 1 \end{cases} \tag{7}$$

and

$$g(x) = \begin{cases} \frac{\beta \log \beta}{\beta-1} \frac{\theta^2}{x^3} e^{-\frac{\theta}{x}} \beta^{-(1+\frac{\theta}{x})e^{-\frac{\theta}{x}}} & \text{if } \beta \neq 1 \\ \frac{\theta^2}{x^3} e^{-\frac{\theta}{x}} & \text{if } \beta = 1 \end{cases}. \tag{8}$$

For $\beta = 1$, we get the ILBE distribution. The survival function $S(x) = 1 - F(x)$ and hazard rate function $h(x) = f(x)/S(x)$ for the BTILBE distribution are provided as follows:

$$S(x) = \begin{cases} \frac{1-\beta^{1-\frac{e^{-\frac{\theta}{x}}(x+\theta)}{x}}}{1-\beta}, & \text{if } \beta \neq 1, \\ 1 - \frac{e^{-\frac{\theta}{x}}(x+\theta)}{x}, & \text{if } \beta = 1. \end{cases} \tag{9}$$

and

$$h(x) = \begin{cases} -\frac{e^{-\frac{\theta}{x}}\beta\theta^2\log(\beta)}{x^3\left(\left(-\beta+\beta^{\frac{e^{-\frac{\theta}{x}}(x+\theta)}{x}}\right)\right)}, & \text{if } \beta \neq 1 \\ \frac{\theta^2}{x^3}\left(e^{-\frac{\theta}{x}}(x+\theta)\right), & \text{if } \beta = 1. \end{cases} \tag{10}$$

Figure 1 illustrates the PDF and HRF of the BTILBE distribution for various parameter combinations. The PDF exhibits a decreasing, unimodal, and right-skewed shape, while the HRF displays diverse patterns, including decreasing, increasing, or upside-down bathtub-shaped behaviors. Figures 2 and 3 present three-dimensional plots of the PDF and HRF, respectively, for various values of the parameter β with a fixed θ. The following observations can be made regarding the PDF of the proposed model:

1) For small θ values (e.g., $\theta = 0.01$), the PDF is sharply peaked near the origin and declines rapidly, indicating a high concentration of probability at smaller x values.
2) For large θ values (e.g., $\theta = 25$), the PDF is flatter with heavier tails, reflecting less concentration near the origin.
3) For moderate θ values (e.g., $\theta = 3, 8$), the PDF strikes a balance between sharpness and spread, exhibiting pronounced right-skewness influenced by β.
4) As β increases, the PDF curves shift, and their slopes adjust, highlighting β's role in controlling skewness and the distribution's spread.

Regarding the HRF, the following patterns are observed:

1) For small θ values (e.g., $\theta = 0.05$), the HRF starts at a high level and decreases rapidly, suggesting a pattern of early failures (infant mortality).
2) For large θ values (e.g., $\theta = 25$), the HRF begins low and increases over time, indicating a wear-out failure pattern.
3) For moderate θ values (e.g., $\theta = 2, 8$), the HRF exhibits non-monotonic behavior, initially rising before stabilizing, resembling bathtub-shaped or unimodal hazard patterns.
4) The parameter β influences the HRF's slope and curvature. For small θ, higher β values lead to a steeper hazard decline, whereas for large θ, higher β amplifies the hazard's growth.

Figure 1
Plot of the PDF for various parameter settings

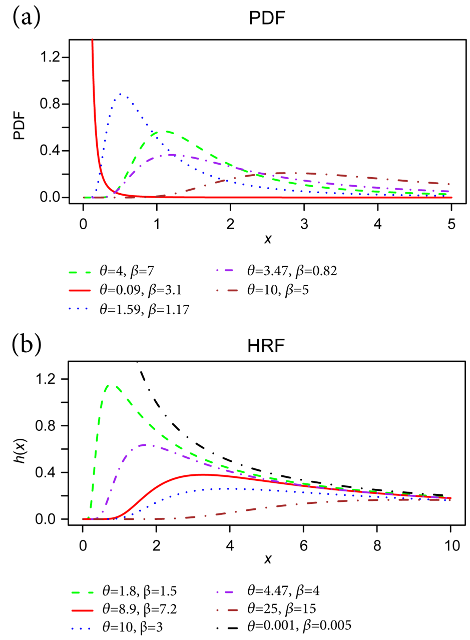

3. Statistical Properties

This section will examine many essential statistical characteristics of the BTILBE distribution, encompassing the moments, inverted moments, incomplete moments, MGF, mean residual life, and mean inactivity time.

3.1. Moments

Moments are key properties in all statistical analyses, particularly in applications. Descriptive statistics, including measures such as the arithmetic mean, variance, skewness, kurtosis, and other parametric indicators, can be calculated to characterize the shape and behavior of a distribution.

The r-th moment of the BTILBE distribution, denoted μ'_r, is given by:

$$\mu'_r = \frac{\beta \log \beta}{\beta - 1}\theta^r \sum_{k=0}^{\infty} \frac{(-\log \beta)^k}{k!} \sum_{m=0}^{k} \binom{k}{m} (1+k)^{r-2-m}\Gamma[m+2-r]. \tag{11}$$

The first four moments of Equation (11) are given by:

$$\mu'_1 = \frac{\beta \log \beta}{\beta - 1}\theta \sum_{k=0}^{\infty} \frac{(-\log \beta)^k}{k!} \sum_{m=0}^{k} \binom{k}{m} (1+k)^{-1-m}\Gamma[m+1],$$

$$\mu'_2 = \frac{\beta \log \beta}{\beta - 1}\theta^2 \sum_{k=0}^{\infty} \frac{(-\log \beta)^k}{k!} \sum_{m=0}^{k} \binom{k}{m} (1+k)^{-m}\Gamma[m],$$

$$\mu'_3 = \frac{\beta \log \beta}{\beta - 1}\theta^3 \sum_{k=0}^{\infty} \frac{(-\log \beta)^k}{k!} \sum_{m=0}^{k} \binom{k}{m} (1+k)^{1-m}\Gamma[m-1],$$

$$\mu'_4 = \frac{\beta \log \beta}{\beta - 1}\theta^4 \sum_{k=0}^{\infty} \frac{(-\log \beta)^k}{k!} \sum_{m=0}^{k} \binom{k}{m} (1+k)^{2-m}\Gamma[m-2].$$

Here, μ'_1 is the mean of the BTILBE distribution, and the variance is obtained by the relation $V(x) = \mu'_2 - (\mu'_1)^2$. Hence, skewness and

Figure 2
3D plots of the PDF for varying parameter β with fixed θ values (0.01, 8, 25, and 3)

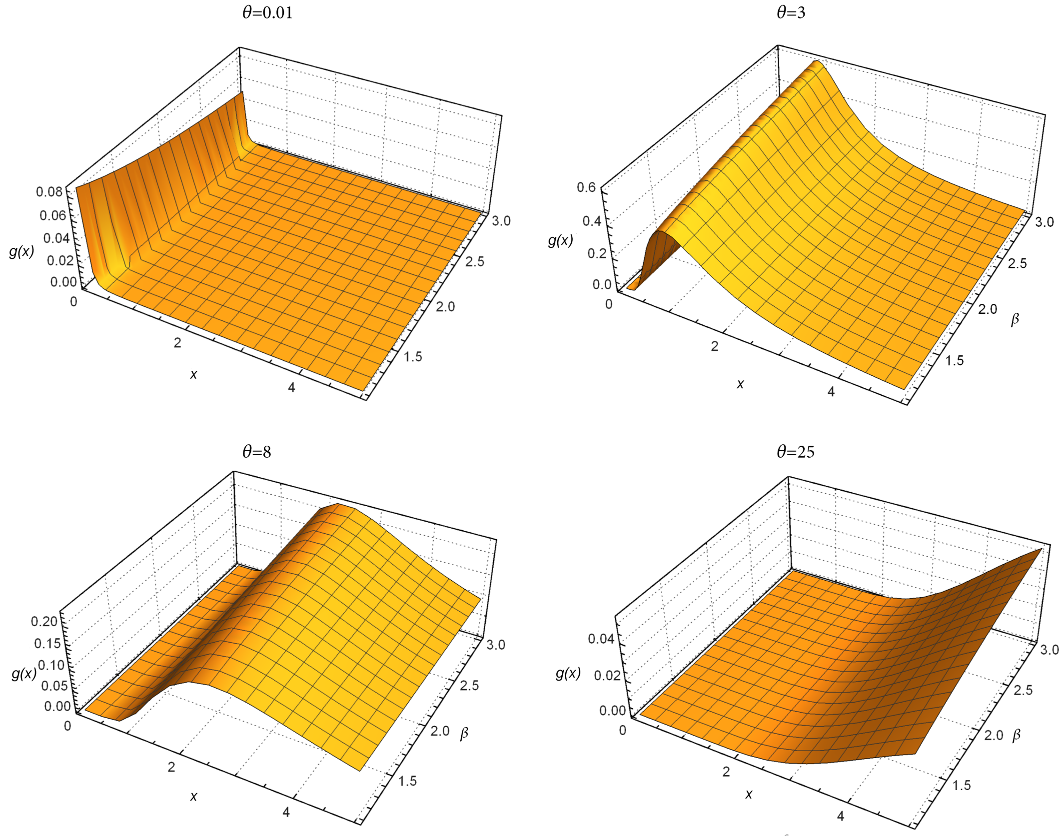

kurtosis can be defined using the relation

$$Skewness = \frac{\mu_3' - 3\mu_1'\mu_2' + 2(\mu_1')^3}{(\mu_2' - (\mu_1')^2)^{3/2}},$$

$$Kurtosis = \frac{\mu_4' - 4\mu_1'\mu_3' + 6(\mu_1')^2\mu_2' - 3(\mu_1')^4}{(\mu_2' - (\mu_1')^2)^2}.$$

Table 1 presents the calculated values of the first three central moments (μ_1, μ_2, and μ_3), variance (V), standard deviation (Sd), skewness (CS), kurtosis (CK), and coefficient of variation ($CV = Sd/\text{A.M.}$) of the BTILBE distribution for various combinations of θ and β. The results reveal that the mean, variance, and higher-order moments increase as the parameter values grow. The distribution exhibits moderate to high positive skewness, confirming its right-skewed nature. Additionally, kurtosis values consistently exceed three, indicating leptokurtic behavior. The coefficient of variation decreases slightly with larger parameter values, suggesting that relative variability stabilizes at higher parameter settings.

The r-th inverted moment of the BTILBE distribution is defined as:

$$\mu_r^* = \frac{\beta\log\beta}{\beta-1}\theta^r \sum_{k=0}^{\infty}\frac{(-\log\beta)^k}{k!}\sum_{m=0}^{k}\binom{k}{m}(1+k)^{r-2-m}\Gamma[r-m-2]. \tag{12}$$

For $n = 1$, this expression yields the harmonic mean of the BTILBE distribution.

The r-th incomplete moment of the BTILBE distribution is given by:

$$\mu_r'(t) = \frac{\beta\log\beta}{\beta-1}\theta^r \sum_{k=0}^{\infty}\frac{(-\log\beta)^k}{k!}\sum_{m=0}^{k}\binom{k}{m}(1+k)^{r-2-m} \times \Gamma_u(m+2-r, \frac{\theta(1+k)}{t}). \tag{13}$$

For the detailed derivation of these results, refer to the Appendix section.

3.2. Moment generating function

The MGF function $M_X(t)$ for the BTILBE distribution is given by:

$$M_X(t) = \mathbb{E}[e^{tX}] = \int_0^\infty e^{tx} g(x)\,dx,$$

using the Taylor series expansion , $e^{tx} = \sum_{r=0}^{\infty}\frac{(tx)^r}{r!}$.

$$M_X(t) = \sum_{r=0}^{\infty}\frac{t^r}{r!}E(x^r). \tag{14}$$

By substituting Equation (11) in Equation (14), we get:

$$M_X(t) = \frac{\beta\log\beta}{\beta-1}\sum_{r=0}^{\infty}\sum_{k=0}^{\infty}\sum_{m=0}^{k}\frac{t^r}{r!}\theta^r\frac{(-\log\beta)^k}{k!}\binom{k}{m}(1+k)^{r-2-m} \times \Gamma[m+2-r]. \tag{15}$$

Figure 3
3D plots of the hazard rate function (HRF) for varying values of the parameter β with fixed values of θ (2, 25, 0.05, and 8). Each subplot corresponds to a specific value of θ

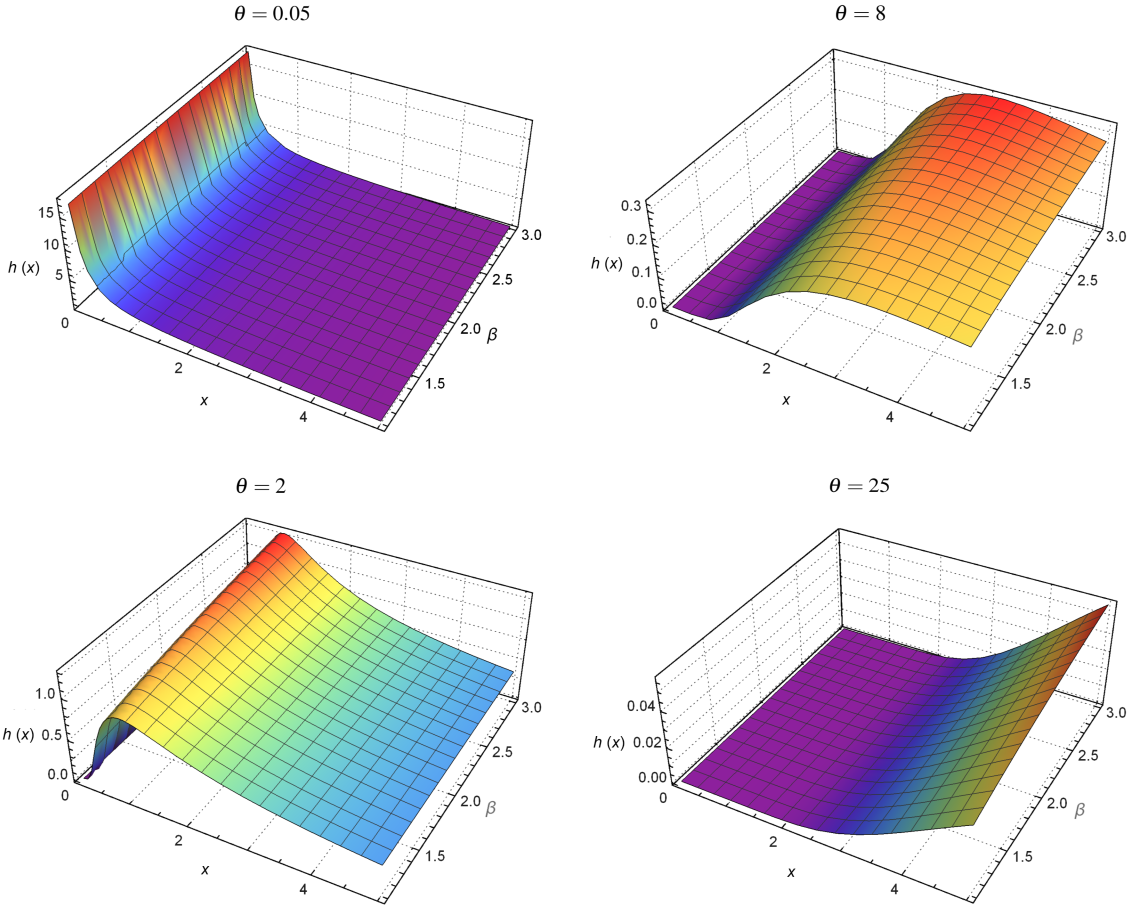

4. Mean Residual Life and Mean Inactivity Time

The mean residual life (MRL) or life expectancy at age t denotes the expected remaining lifespan of a unit that has survived to age t. This measure is widely used in fields such as biomedical sciences, life insurance, product maintenance, quality control, economics, social studies, demography, and product technology. The MRL is expressed as:

$$\mu(t) = E(X - t \mid X > t) = \frac{1 - \Psi_1(t)}{S(t)} - t, \quad \text{for } t > 0, \tag{16}$$

where $\Psi_1(t) = \int_0^t v f(v)\, dv$ is the first incomplete moment of X. The first incomplete moment for the BTILBE distribution, as derived from Equation (13), is:

$$\Psi_1(t) = \frac{\theta\beta \log\beta}{\beta - 1} \sum_{k=0}^{\infty} \frac{(-\log\beta)^k}{k!} \sum_{m=0}^{k} \binom{k}{m} (1+k)^{-1-m} \times \Gamma_u(m+1, \frac{\theta(1+k)}{t}),$$

where $\Gamma_u(m+1, a) = \int_a^\infty u^m e^{-u}\, du$ is the upper incomplete gamma function. By substituting $\Psi_1(t)$ into Equation (16), the MRL is:

$$\mu(t) = \frac{1 - \frac{\theta\beta\log\beta}{\beta-1} \sum_{k=0}^{\infty} \frac{(-\log\beta)^k}{k!} \sum_{m=0}^{k} \binom{k}{m} (1+k)^{-1-m} \Gamma_u(m+1, \frac{\theta(1+k)}{t})}{S(t)} - t. \tag{17}$$

The mean inactivity time (MIT) represents the waiting time elapsed since the failure of an item under the condition that this failure had occurred in $(0, t)$. The MIT of X is given (for $t > 0$) by:

$$M(t) = t - \frac{\frac{\theta\beta\log\beta}{\beta-1}}{F(t)} \sum_{k=0}^{\infty} \frac{(-\log\beta)^k}{k!} \sum_{m=0}^{k} \binom{k}{m} (1+k)^{-1-m} \Gamma_u(m+1, \frac{\theta(1+k)}{t}).$$

5. Entropy Measures

The entropy of a random variable quantifies the degree of uncertainty in its outcomes and functions as a measure of variability. It has been used in a variety of scientific and engineering disciplines.

5.1. Shannon entropy

The Shannon entropy (SHE) of a random variable X is symbolized by $E[-\log(g(x))]$. The SHE for the BTILBE distribution when $\beta \neq 1$ is provided via:

$$H = -\int_0^\infty g(x) \log g(x)\, dx,$$

Table 1
Results of μ_1', μ_2', μ_3', V, Sd, CS, CK, and CV for the BTILBE model

θ	β	μ_1'	μ_2'	μ_3'	V	Sd	CS	CK	CV
1.5	0.1	2.49021	19.08517	530.52310	12.88403	3.58943	9.05648	139.86199	1.44142
	0.2	2.17461	15.35612	418.27860	10.62717	3.25994	9.77561	165.44542	1.49909
	0.3	1.99419	13.32800	358.18860	9.35120	3.05797	10.29224	185.12885	1.53344
	0.4	1.86950	11.97179	318.41980	8.47676	2.91149	10.71087	201.89321	1.55736
	0.5	1.77524	10.97195	289.32980	7.82047	2.79651	11.06928	216.83380	1.57529
	0.6	1.70009	10.19087	266.74860	7.30058	2.70196	11.38608	230.49583	1.58931
	0.7	1.63799	9.55660	248.51060	6.87359	2.62175	11.67200	243.19714	1.60059
	0.8	1.58537	9.02706	233.35470	6.51367	2.55219	11.93388	255.14175	1.60984
	0.9	1.53989	8.57556	220.48610	6.20429	2.49084	12.17638	266.46997	1.61754
2	0.1	3.32028	31.03686	922.36410	20.01262	4.47355	7.66713	96.20018	1.34734
	0.2	2.89948	25.02517	727.88850	16.61816	4.07654	8.25100	113.12233	1.40595
	0.3	2.65892	21.74948	623.67580	14.67960	3.83140	8.67270	126.14307	1.44096
	0.4	2.49267	19.55637	554.66410	13.34298	3.65280	9.01526	137.22972	1.46542
	0.5	2.36699	17.93810	504.16110	12.33547	3.51219	9.30897	147.10610	1.48382
	0.6	2.26678	16.67297	464.94410	11.53468	3.39628	9.56879	156.13330	1.49828
	0.7	2.18399	15.64505	433.26070	10.87524	3.29776	9.80342	164.52182	1.50997
	0.8	2.11382	14.78638	406.92500	10.31814	3.21219	10.01840	172.40701	1.51961
	0.9	2.05319	14.05394	384.55890	9.83835	3.13662	10.21751	179.88199	1.52768
2.5	0.1	4.15035	45.00800	1410.78080	27.78262	5.27092	6.78344	72.84960	1.27000
	0.2	3.62436	36.35934	1114.37230	23.22339	4.81907	7.27564	85.17296	1.32963
	0.3	3.32366	31.63857	955.38100	20.59189	4.53783	7.63405	94.66627	1.36531
	0.4	3.11584	28.47465	850.02890	18.76622	4.33200	7.92619	102.74961	1.39032
	0.5	2.95873	26.13804	772.89710	17.38393	4.16940	8.17726	109.95098	1.40919
	0.6	2.83348	24.31014	712.98050	16.28157	4.03504	8.39967	116.53197	1.42406
	0.7	2.72999	22.82414	664.55940	15.37131	3.92063	8.60070	122.64585	1.43613
	0.8	2.64228	21.58224	624.30080	14.60062	3.82108	8.78502	128.39140	1.44613
	0.9	2.56649	20.52246	590.10280	13.93561	3.73304	8.95581	133.83634	1.45454
3	0.1	4.98042	60.73052	1990.11520	35.92596	5.99383	6.17552	58.61998	1.20348
	0.2	4.34923	49.14751	1573.48920	30.23174	5.49834	6.59811	68.13843	1.26421
	0.3	3.98839	42.81496	1349.79070	26.90774	5.18727	6.90935	75.48564	1.30059
	0.4	3.73900	38.56622	1201.46850	24.58607	4.95843	7.16451	81.74770	1.32614
	0.5	3.55048	35.42611	1092.82670	22.82019	4.77705	7.38444	87.32754	1.34547
	0.6	3.40017	32.96815	1008.40210	21.40700	4.62677	7.57967	92.42695	1.36075
	0.7	3.27599	30.96890	940.15420	20.23683	4.49854	7.75637	97.16412	1.37319
	0.8	3.17073	29.29732	883.39630	19.24379	4.38678	7.91854	101.61528	1.38352
	0.9	3.07978	27.87032	835.17200	18.38526	4.28780	8.06892	105.83292	1.39224

where the PDF is defined in Equation (8). Now, by expanding $\log g(x)$, we get:

$$\log g(x) = \log\left(\frac{\beta\log\beta}{\beta-1}\right) + 2\log\theta - 3\log x - \frac{\theta}{x} - \left(1+\frac{\theta}{x}\right)e^{-\frac{\theta}{x}}\log\beta. \tag{18}$$

By substituting into the SHE definition, we have:

$$H = -\int_0^\infty g(x)\left[\log\left(\frac{\beta\log\beta}{\beta-1}\right) + 2\log\theta - 3\log x - \frac{\theta}{x} - \left(1+\frac{\theta}{x}\right)e^{-\frac{\theta}{x}}\log\beta\right]dx.$$

Separating terms yields:

$$H = -\log\left(\frac{\beta\log\beta}{\beta-1}\right) - 2\log\theta + 3\mathbb{E}[\log x] + \mathbb{E}\left[\frac{\theta}{x}\right] - \log\beta\int_0^\infty g(x)\left(1+\frac{\theta}{x}\right)e^{-\frac{\theta}{x}}dx. \tag{19}$$

5.2. Tsallis entropy

Tsallis entropy (TE) is provided via:

$$H_T = \int_0^\infty x g(x)\log g(x)dx.$$

By substituting Equation (8) and Equation (18) into the TE formula, we obtain the following:

$$H_T = \int_0^\infty x g(x) \left[\log\left(\frac{\beta\log\beta}{\beta-1}\right) + 2\log\theta - 3\log x - \frac{\theta}{x} - \left(1+\frac{\theta}{x}\right)e^{-\frac{\theta}{x}}\log\beta\right] dx.$$

Breaking this into individual terms:

$$H_T = \log\left(\frac{\beta\log\beta}{\beta-1}\right)E[X] + 2\log\theta E[X] - 3E[X\log X] - E[\theta] - \log\beta E\left[X(1+\frac{\theta}{X})e^{-\frac{\theta}{X}}\right], \tag{20}$$

Table 2
SHE, TE, and RE for different values of β, θ, and α = 1.2

β	θ	SHE (H)	TE (H_T)	RE (H_α)
	0.1	0.73677	3.90921	0.67652
	0.2	0.67491	3.31591	0.61355
	0.3	0.63398	2.97684	0.57179
	0.4	0.60287	2.74221	0.54006
1.5	0.5	0.57763	2.56457	0.51434
	0.6	0.55633	2.42269	0.49267
	0.7	0.53788	2.30529	0.47393
	0.8	0.52160	2.20563	0.45742
	0.9	0.50703	2.11940	0.44267
	0.1	0.86170	5.62712	0.80146
	0.2	0.79985	4.78347	0.73849
	0.3	0.75892	4.30132	0.69673
	0.4	0.72781	3.96772	0.66500
2	0.5	0.70257	3.71515	0.63928
	0.6	0.68127	3.51347	0.61761
	0.7	0.66282	3.34659	0.59887
	0.8	0.64654	3.20494	0.58236
	0.9	0.63197	3.08239	0.56761
	0.1	0.95862	7.43610	0.89837
	0.2	0.89676	6.33058	0.83540
	0.3	0.85583	5.69875	0.79364
	0.4	0.82472	5.26160	0.76191
2.5	0.5	0.79948	4.93067	0.73619
	0.6	0.77818	4.66642	0.71452
	0.7	0.75973	4.44780	0.69578
	0.8	0.74345	4.26224	0.67927
	0.9	0.72888	4.10170	0.66452
	0.1	1.03780	9.31768	0.97755
	0.2	0.97594	7.94107	0.91458
	0.3	0.93501	7.15430	0.87282
	0.4	0.90390	6.60998	0.84109
3	0.5	0.87866	6.19793	0.81537
	0.6	0.85736	5.86894	0.79370
	0.7	0.83891	5.59675	0.77496
	0.8	0.82263	5.36575	0.75845
	0.9	0.80806	5.16590	0.74370

where $E[X]$ and $E[X \log X]$ can be found from the given moments of the BTILBE distribution.

5.3. Rényi entropy

The Rényi entropy (RE) of order α is provided via:

$$H_\alpha = \frac{1}{1-\alpha} \log \left(\int_0^\infty g(x)^\alpha \, dx \right).$$

The PDF raised to the power α is:

$$g(x)^\alpha = \left(\frac{\beta \log \beta}{\beta - 1} \frac{\theta^2}{x^3} e^{-\frac{\theta}{x}} \beta^{-\left(1+\frac{\theta}{x}\right)e^{-\frac{\theta}{x}}} \right)^\alpha.$$

By simplifying this, we get:

$$g(x)^\alpha = \left(\frac{\beta \log \beta}{\beta - 1} \right)^\alpha \frac{\theta^{2\alpha}}{x^{3\alpha}} e^{-\frac{\alpha\theta}{x}} \beta^{-\alpha\left(1+\frac{\theta}{x}\right)e^{-\frac{\theta}{x}}}.$$

By substituting into the RE definition, the RE becomes:

$$H_\alpha = \frac{1}{1-\alpha} \log \left[\left(\frac{\beta \log \beta}{\beta - 1} \right)^\alpha \theta^{2\alpha} \int_0^\infty x^{-3\alpha} e^{-\frac{\alpha\theta}{x}} \beta^{-\alpha\left(1+\frac{\theta}{x}\right)e^{-\frac{\theta}{x}}} dx \right]. \tag{21}$$

As shown in Table 2, the Shannon entropy (SHE) decreases steadily as the parameter θ increases. Similarly, both the Tsallis entropy (TE) and the Rényi entropy (RE) exhibit a decreasing trend with increasing θ. For a fixed value of θ, higher values of β result in increased entropy measures. Specifically, the Shannon entropy remains within the interval $(0.5, 1.05)$, while the Tsallis and Rényi entropies tend to reach higher values, suggesting greater sensitivity to changes in the parameters.

6. Maximum Likelihood Estimation

The maximum likelihood estimate (MLE) method is the most commonly used way to estimate parameters. It is popular because it is reliable, efficient, and easy to understand. Consider a random sample $X = (x_1, x_2, \ldots, x_q)$ from the BTILBE distribution. Then, the log-likelihood functions $\log L$ of the BTILBE distribution, corresponding to Equation (8), are given by Equations (23) and (24):

$$\ell(\beta, \theta; \mathbf{x}) = \sum_{i=1}^{n} \Bigg[\log \beta + \log(\log \beta) - \log(\beta - 1) + 2\log\theta - 3\log x_i - \frac{\theta}{x_i} - \left(1 + \frac{\theta}{x_i}\right) e^{-\frac{\theta}{x_i}} \log \beta \Bigg]. \tag{22}$$

To obtain the maximum likelihood estimates (MLEs) for the parameters β and θ, we first compute the partial derivatives of Equation (22) with respect to β and θ and then set them equal to zero. This results in the following two equations:

$$\frac{\partial \ell}{\partial \beta} = \sum_{i=1}^{n} \left[\frac{1}{\beta} \left(1 - \left(1 + \frac{\theta}{x_i}\right) e^{-\frac{\theta}{x_i}} \right) + \frac{1}{\beta \log \beta} - \frac{1}{\beta - 1} \right]. \tag{23}$$

$$\frac{\partial \ell}{\partial \theta} = \sum_{i=1}^{n} \left[\frac{2}{\theta} - \frac{1}{x_i} + \log \beta \frac{\theta}{x_i^2} e^{-\frac{\theta}{x_i}} \right]. \tag{24}$$

The MLEs of the parameters β and θ, denoted as $\hat{\beta}_1$ and $\hat{\theta}_1$, respectively, are obtained by solving the nonlinear system of equations $\frac{\partial \ell(\beta,\theta)}{\partial \beta} = 0$ and $\frac{\partial \ell(\beta,\theta)}{\partial \theta} = 0$. While these equations cannot be solved analytically, we use R software to address them numerically through iterative methods, such as the Newton-Raphson technique via the optim() function.

7. Simulation

This study conducts a simulation to evaluate the performance of the maximum likelihood estimators (MLEs) for the parameters (θ, β) of the BTILBE distribution. Using an R package, we compute key performance metrics, including the mean, bias, relative bias (RBias), mean squared error (MSE), root mean squared error (RMSE), average interval length (AIL) at a 95% confidence level, and coverage probability (CP) at a 95% confidence level for the estimated θ and β. The simulation involves generating 1,000 random samples from the BTILBE distribution with sample sizes of $n = (30, 50, 100, 150, 200, 250, 300, 350, 400, 450)$. The parameters are configured across 10 distinct sets as specified.

- Set 1 = (θ = 1.7 and β = 1.3)

Table 3
Simulation values for all parameter sets

Set	N	Parameter	Mean	RBias	Bias	MSE	RMSE	AIL	CP
Set 1 (θ = 1.7, β = 1.3)	30	θ	1.71386	0.00815	0.01386	0.01798	0.13409	0.52188	96.4
		β	2.02800	0.56000	0.72800	0.56771	0.75346	0.76176	96.6
	50	θ	1.71145	0.00673	0.01144	0.01223	0.11061	0.43145	96.2
		β	2.00003	0.53848	0.70003	0.51555	0.71802	0.62645	96.6
	70	θ	1.70719	0.00423	0.00719	0.00842	0.09176	0.35889	96.6
		β	1.99956	0.53812	0.69956	0.50135	0.70806	0.49889	96.3
	100	θ	1.70677	0.00398	0.00677	0.00575	0.07586	0.29708	96.8
		β	1.99654	0.53580	0.69654	0.50062	0.70755	0.41575	96.3
	150	θ	1.70672	0.00395	0.00672	0.00432	0.06571	0.25616	97.4
		β	1.98913	0.53010	0.68913	0.48295	0.69495	0.36313	96.4
	200	θ	1.70629	0.00370	0.00629	0.00336	0.05800	0.22596	97.5
		β	1.98875	0.52981	0.68875	0.48052	0.69319	0.31446	96.3
	250	θ	1.70542	0.00319	0.00542	0.00260	0.05096	0.19835	96.9
		β	1.98789	0.52914	0.68789	0.47962	0.69254	0.29388	97.4
	300	θ	1.70507	0.00298	0.00507	0.00248	0.04983	0.19443	96.5
		β	1.98488	0.52683	0.68488	0.47293	0.68770	0.27003	97.3
	350	θ	1.70503	0.00296	0.00503	0.00191	0.04373	0.17035	97.3
		β	1.98483	0.52679	0.68483	0.47275	0.68757	0.24397	97.1
	400	θ	1.70443	0.00261	0.00443	0.00187	0.04324	0.16823	96.9
		β	1.98411	0.52624	0.68411	0.47216	0.68714	0.23681	97.3
	450	θ	1.70412	0.00242	0.00412	0.00160	0.03998	0.15584	97.2
		β	1.98393	0.52610	0.68393	0.47140	0.68659	0.22086	96.7
Set 2 (θ = 2.1, β = 1.1)	30	θ	2.11937	0.00922	0.01937	0.03738	0.19335	0.75447	96.5
		β	1.71118	0.55561	0.61118	0.40092	0.63318	0.64899	95.7
	50	θ	2.11408	0.00671	0.01408	0.02505	0.15827	0.61944	97.0
		β	1.70083	0.54621	0.60083	0.37911	0.61572	0.52784	96.6
	70	θ	2.11202	0.00572	0.01202	0.01737	0.13180	0.51578	97.7
		β	1.69444	0.54040	0.59444	0.36594	0.60493	0.44000	96.1
	100	θ	2.11169	0.00557	0.01169	0.01232	0.11101	0.43283	97.2
		β	1.68511	0.53192	0.58511	0.35017	0.59175	0.34668	97.0
	150	θ	2.11055	0.00502	0.01055	0.00956	0.09776	0.37942	96.9
		β	1.68072	0.52793	0.58072	0.34308	0.58573	0.31129	96.3
	200	θ	2.11020	0.00486	0.01020	0.00750	0.08659	0.33762	96.9
		β	1.68053	0.52775	0.58053	0.34133	0.58423	0.27180	97.7
	250	θ	2.10938	0.00447	0.00938	0.00563	0.07504	0.29071	97.3
		β	1.68033	0.52757	0.58033	0.34036	0.58340	0.24023	97.0
	300	θ	2.10899	0.00428	0.00899	0.00502	0.07082	0.27600	96.9
		β	1.68011	0.52737	0.58011	0.34006	0.58314	0.22686	96.9
	350	θ	2.10865	0.00412	0.00865	0.00431	0.06569	0.25519	97.4
		β	1.67992	0.52720	0.57992	0.34005	0.58314	0.20806	97.5
	400	θ	2.10795	0.00379	0.00795	0.00379	0.06156	0.23785	97.3
		β	1.67795	0.52541	0.57795	0.33660	0.58017	0.19874	97.5
	450	θ	2.10677	0.00323	0.00677	0.00370	0.06087	0.23723	96.9
		β	1.67737	0.52488	0.57737	0.33559	0.57930	0.18538	96.6
Set 3 (θ = 1.8, β = 0.8)	30	θ	1.84001	0.02223	0.04001	0.09366	0.30603	0.31373	96.1
		β	1.26406	0.58007	0.46406	0.24005	0.48995	1.19369	96.8
	50	θ	1.83189	0.01771	0.03188	0.05301	0.23024	0.30188	96.5
		β	1.24735	0.55918	0.44735	0.21433	0.46296	0.88923	96.4
	70	θ	1.82296	0.01276	0.02296	0.03852	0.19627	0.29199	96.7
		β	1.23689	0.54611	0.43689	0.20040	0.44766	0.76446	97.3
	100	θ	1.81588	0.00882	0.01588	0.02426	0.15574	0.27631	97.2
		β	1.23226	0.54032	0.43226	0.19324	0.43960	0.61634	96.7
	150	θ	1.81319	0.00733	0.01319	0.01601	0.12653	0.25267	97.0
		β	1.22545	0.53181	0.42545	0.18468	0.42975	0.60761	96.2
	200	θ	1.81198	0.00666	0.01198	0.01265	0.11248	0.21699	96.7
		β	1.22489	0.53111	0.42489	0.18346	0.42832	0.49400	96.9

Table 3
(continued)

Set	N	Parameter	Mean	RBias	Bias	MSE	RMSE	AIL	CP
	250	θ	1.80996	0.00553	0.00996	0.00925	0.09619	0.19431	96.2
		β	1.22375	0.52969	0.42375	0.18262	0.42735	0.46748	97.5
	300	θ	1.80966	0.00537	0.00966	0.00787	0.08871	0.17315	97.1
		β	1.22307	0.52883	0.42307	0.18018	0.42447	0.43809	96.2
	350	θ	1.80922	0.00512	0.00922	0.00749	0.08654	0.16686	97.1
		β	1.22133	0.52666	0.42133	0.17946	0.42363	0.38273	96.6
	400	θ	1.80876	0.00487	0.00876	0.00602	0.07758	0.14952	96.5
		β	1.22113	0.52641	0.42113	0.17876	0.42280	0.37521	96.7
	450	θ	1.80831	0.00462	0.00831	0.00563	0.07502	0.14707	97.4
		β	1.22047	0.52558	0.42046	0.17841	0.42239	0.34636	97.6
Set 4 (θ = 0.8, β = 0.5)	30	θ	0.83612	0.04516	0.03612	0.04815	0.21943	0.84884	95.0
		β	0.78990	0.57979	0.28990	0.09393	0.30649	0.39012	95.6
	50	θ	0.82411	0.03013	0.02411	0.02590	0.16093	0.62441	96.3
		β	0.77462	0.54923	0.27462	0.08029	0.28335	0.27384	96.1
	70	θ	0.82344	0.02930	0.02344	0.01882	0.13717	0.52961	96.6
		β	0.77130	0.54261	0.27130	0.07727	0.27797	0.23736	96.5
	100	θ	0.81762	0.02203	0.01762	0.01388	0.11780	0.45679	95.9
		β	0.76678	0.53356	0.26678	0.07369	0.27147	0.19702	96.2
	150	θ	0.80918	0.01148	0.00918	0.00888	0.09424	0.36788	96.8
		β	0.76666	0.53331	0.26666	0.07268	0.26959	0.15547	97.3
	200	θ	0.80910	0.01137	0.00910	0.00623	0.07891	0.30738	96.6
		β	0.76582	0.53164	0.26582	0.07189	0.26813	0.13771	96.4
	250	θ	0.80846	0.01058	0.00846	0.00529	0.07272	0.28327	97.1
		β	0.76436	0.52873	0.26436	0.07054	0.26560	0.12345	96.9
	300	θ	0.80782	0.00978	0.00782	0.00379	0.06160	0.23968	97.1
		β	0.76390	0.52780	0.26390	0.07048	0.26547	0.11325	96.7
	350	θ	0.80769	0.00962	0.00769	0.00339	0.05827	0.22735	96.8
		β	0.76348	0.52697	0.26348	0.07041	0.26536	0.10047	96.7
	400	θ	0.80728	0.00910	0.00728	0.00292	0.05404	0.21000	96.8
		β	0.76321	0.52643	0.26321	0.06984	0.26427	0.09271	96.9
	450	θ	0.80588	0.00734	0.00588	0.00255	0.05054	0.19583	96.4
		β	0.76245	0.52489	0.26245	0.06930	0.26325	0.08053	96.5
Set 5 (θ = 1.5, β = 0.2)	30	θ	1.72039	0.14693	0.22039	0.94376	0.97147	3.57573	96.2
		β	0.30985	0.54924	0.10985	0.01291	0.11363	0.11396	95.9
	50	θ	1.70738	0.13825	0.20738	0.65361	0.80846	3.06462	95.3
		β	0.30801	0.54007	0.10801	0.01223	0.11059	0.09301	96.4
	70	θ	1.61965	0.07977	0.11965	0.34950	0.59119	2.27059	95.0
		β	0.30778	0.53891	0.10778	0.01202	0.10962	0.07840	95.9
	100	θ	1.58644	0.05762	0.08644	0.24058	0.49049	1.89353	95.1
		β	0.30689	0.53444	0.10689	0.01167	0.10804	0.06171	96.4
	150	θ	1.56818	0.04545	0.06818	0.15140	0.38910	1.50239	95.3
		β	0.30636	0.53179	0.10636	0.01147	0.10711	0.05103	97.1
	200	θ	1.56487	0.04325	0.06487	0.12913	0.35935	1.39208	96.6
		β	0.30594	0.52968	0.10594	0.01139	0.10673	0.04984	97.2
	250	θ	1.55679	0.03786	0.05679	0.10122	0.31816	1.22975	96.3
		β	0.30562	0.52812	0.10562	0.01128	0.10621	0.04373	97.2
	300	θ	1.55607	0.03738	0.05607	0.08873	0.29787	1.15199	95.6
		β	0.30549	0.52744	0.10549	0.01123	0.10597	0.04269	96.9
	350	θ	1.55388	0.03592	0.05388	0.08182	0.28605	1.09261	96.2
		β	0.30541	0.52703	0.10541	0.01120	0.10585	0.03706	97.0
	400	θ	1.54946	0.03297	0.04946	0.06720	0.25923	0.99199	95.7
		β	0.30508	0.52538	0.10508	0.01113	0.10550	0.03590	96.9
	450	θ	1.53422	0.02281	0.03422	0.05889	0.24267	0.94220	96.5
		β	0.30474	0.52370	0.10474	0.01105	0.10514	0.03417	96.6

Table 3
(continued)

Set	N	Parameter	Mean	RBias	Bias	MSE	RMSE	AIL	CP
Set 6 (θ = 0.7, β = 1.3)	30	θ	0.70536	0.00766	0.00536	0.00276	0.05250	0.20571	96.7
		β	2.02268	0.55591	0.72268	0.55729	0.74652	0.73389	96.5
	50	θ	0.70347	0.00496	0.00347	0.00195	0.04419	0.17203	96.1
		β	2.01068	0.54668	0.71068	0.52975	0.72784	0.61622	96.9
	70	θ	0.70296	0.00424	0.00296	0.00136	0.03685	0.14407	96.5
		β	2.00136	0.53951	0.70136	0.50877	0.71328	0.50925	96.7
	100	θ	0.70295	0.00421	0.00295	0.00092	0.03033	0.11816	97.2
		β	1.99158	0.53198	0.69158	0.48950	0.69964	0.41538	96.8
	150	θ	0.70246	0.00351	0.00246	0.00069	0.02625	0.10255	96.8
		β	1.98859	0.52968	0.68859	0.48225	0.69444	0.35289	97.4
	200	θ	0.70234	0.00334	0.00234	0.00057	0.02381	0.09319	96.7
		β	1.98721	0.52863	0.68721	0.47871	0.69189	0.31501	97.1
	250	θ	0.70231	0.00330	0.00231	0.00048	0.02193	0.08546	97.3
		β	1.98690	0.52839	0.68690	0.47627	0.69013	0.28436	97.3
	300	θ	0.70219	0.00313	0.00219	0.00040	0.01995	0.07798	96.7
		β	1.98657	0.52813	0.68657	0.47608	0.68999	0.27454	97.1
	350	θ	0.70172	0.00246	0.00172	0.00035	0.01860	0.07265	96.9
		β	1.98462	0.52663	0.68462	0.47184	0.68691	0.25561	96.4
	400	θ	0.70167	0.00239	0.00167	0.00033	0.01825	0.07061	96.7
		β	1.98291	0.52531	0.68291	0.47162	0.68675	0.23633	97.1
	450	θ	0.70147	0.00210	0.00147	0.00027	0.01658	0.06446	96.9
		β	1.98151	0.52424	0.68151	0.46808	0.68417	0.21954	97.1
Set 7 (θ = 1.1, β = 0.9)	30	θ	1.11018	0.00925	0.01018	0.01405	0.11855	0.46366	97.0
		β	1.39748	0.55275	0.49748	0.26334	0.51317	0.49390	96.6
	50	θ	1.10873	0.00793	0.00873	0.01066	0.10324	0.40290	96.7
		β	1.39114	0.54571	0.49114	0.25288	0.50287	0.42355	96.6
	70	θ	1.10754	0.00686	0.00754	0.00753	0.08676	0.33922	97.2
		β	1.38379	0.53754	0.48379	0.23958	0.48947	0.35617	96.6
	100	θ	1.10727	0.00661	0.00727	0.00472	0.06869	0.26930	96.8
		β	1.37949	0.53277	0.47949	0.23816	0.48802	0.29181	96.9
	150	θ	1.10678	0.00616	0.00678	0.00367	0.06057	0.23569	97.5
		β	1.37700	0.53000	0.47700	0.23110	0.48073	0.25219	96.7
	200	θ	1.10639	0.00581	0.00639	0.00307	0.05539	0.21614	96.3
		β	1.37641	0.52934	0.47641	0.22984	0.47941	0.22768	96.3
	250	θ	1.10567	0.00516	0.00567	0.00244	0.04944	0.19179	96.8
		β	1.37552	0.52835	0.47552	0.22949	0.47905	0.20072	97.3
	300	θ	1.10553	0.00503	0.00553	0.00198	0.04446	0.17418	97.0
		β	1.37472	0.52747	0.47472	0.22798	0.47747	0.18827	97.1
	350	θ	1.10551	0.00501	0.00551	0.00176	0.04196	0.16315	97.4
		β	1.37314	0.52571	0.47313	0.22556	0.47493	0.17084	97.4
	400	θ	1.10214	0.00194	0.00213	0.00169	0.04112	0.15931	97.4
		β	1.37293	0.52547	0.47293	0.22544	0.47480	0.16310	97.1
	450	θ	1.10184	0.00167	0.00184	0.00144	0.03795	0.14718	96.7
		β	1.37191	0.52435	0.47191	0.22443	0.47374	0.15583	97.4
Set 8 (θ = 2.5, β = 0.5)	30	θ	2.58636	0.03454	0.08636	0.29350	0.54176	2.09754	95.2
		β	0.77643	0.55285	0.27643	0.08188	0.28614	0.28989	96.7
	50	θ	2.55247	0.02099	0.05247	0.17545	0.41886	1.62979	96.0
		β	0.77401	0.54802	0.27401	0.07838	0.27996	0.22508	96.6
	70	θ	2.54953	0.01981	0.04953	0.12179	0.34898	1.35480	95.8
		β	0.76837	0.53674	0.26837	0.07445	0.27285	0.19310	96.4
	100	θ	2.53090	0.01236	0.03090	0.08003	0.28290	1.10545	96.0
		β	0.76634	0.53267	0.26634	0.07216	0.26862	0.16324	95.7
	150	θ	2.52854	0.01142	0.02854	0.06150	0.24798	0.96498	96.9
		β	0.76493	0.52986	0.26493	0.07192	0.26818	0.13709	96.8
	200	θ	2.52412	0.00965	0.02412	0.04999	0.22358	0.87192	96.2
		β	0.76480	0.52960	0.26480	0.07107	0.26659	0.12107	97.2

Table 3
(continued)

Set	N	Parameter	Mean	RBias	Bias	MSE	RMSE	AIL	CP
	250	θ	2.52367	0.00947	0.02367	0.03916	0.19788	0.77061	97.2
		β	0.76436	0.52872	0.26436	0.07041	0.26535	0.11222	97.4
	300	θ	2.52343	0.00937	0.02343	0.03357	0.18322	0.71621	96.3
		β	0.76378	0.52757	0.26378	0.07040	0.26533	0.10312	97.0
	350	θ	2.51485	0.00594	0.01485	0.02998	0.17316	0.66981	97.2
		β	0.76362	0.52725	0.26362	0.07019	0.26493	0.09978	96.6
	400	θ	2.51398	0.00559	0.01398	0.02491	0.15783	0.61655	97.3
		β	0.76349	0.52698	0.26349	0.06989	0.26437	0.08982	96.7
	450	θ	2.51276	0.00510	0.01276	0.02385	0.15445	0.60365	97.0
		β	0.76259	0.52518	0.26259	0.06960	0.26382	0.08480	96.4
Set 9 (θ = 2.2, β = 1.1)	30	θ	2.22200	0.01000	0.02200	0.03825	0.19558	0.76217	96.1
		β	1.70690	0.55173	0.60690	0.39372	0.62747	0.62496	96.4
	50	θ	2.21715	0.00779	0.01715	0.02635	0.16232	0.63305	96.8
		β	1.69358	0.53962	0.59358	0.36993	0.60822	0.52029	96.1
	70	θ	2.21196	0.00544	0.01196	0.01906	0.13804	0.54075	97.1
		β	1.68990	0.53627	0.58990	0.35984	0.59987	0.42711	96.9
	100	θ	2.21162	0.00528	0.01162	0.01316	0.11472	0.44759	97.1
		β	1.68867	0.53515	0.58867	0.35454	0.59543	0.35100	97.1
	150	θ	2.20935	0.00425	0.00935	0.00887	0.09419	0.36642	96.8
		β	1.68475	0.53159	0.58475	0.34690	0.58898	0.29797	97.3
	200	θ	2.20838	0.00381	0.00838	0.00798	0.08933	0.34904	96.7
		β	1.67998	0.52726	0.57998	0.34131	0.58422	0.27648	97.2
	250	θ	2.20806	0.00366	0.00806	0.00665	0.08158	0.31889	97.4
		β	1.67926	0.52660	0.57926	0.34041	0.58345	0.24917	97.8
	300	θ	2.20768	0.00349	0.00768	0.00528	0.07269	0.28318	97.1
		β	1.67904	0.52640	0.57904	0.33843	0.58175	0.21984	96.9
	350	θ	2.20729	0.00331	0.00729	0.00479	0.06918	0.26882	96.7
		β	1.67867	0.52606	0.57867	0.33761	0.58104	0.20568	97.1
	400	θ	2.20673	0.00306	0.00672	0.00432	0.06574	0.25587	96.5
		β	1.67790	0.52537	0.57790	0.33627	0.57988	0.19287	97.2
	450	θ	2.20660	0.00300	0.00660	0.00380	0.06166	0.24014	96.9
		β	1.67699	0.52453	0.57699	0.33533	0.57908	0.18786	97.1
Set 10 (θ = 1.4, β = 0.6)	30	θ	1.43682	0.02630	0.03682	0.05792	0.24067	0.93276	96.5
		β	0.93508	0.55847	0.33508	0.12003	0.34645	0.34527	96.5
	50	θ	1.43311	0.02365	0.03311	0.04262	0.20645	0.79936	96.8
		β	0.92686	0.54476	0.32686	0.11231	0.33513	0.29023	96.2
	70	θ	1.43284	0.02346	0.03284	0.02860	0.16911	0.65041	96.4
		β	0.92027	0.53378	0.32027	0.10618	0.32586	0.23566	97.2
	100	θ	1.42156	0.01540	0.02156	0.01794	0.13393	0.51877	97.3
		β	0.91853	0.53088	0.31853	0.10376	0.32212	0.18810	97.3
	150	θ	1.42097	0.01498	0.02097	0.01352	0.11628	0.45362	96.8
		β	0.91709	0.52849	0.31709	0.10228	0.31981	0.17023	97.1
	200	θ	1.41681	0.01200	0.01681	0.01076	0.10375	0.40374	95.7
		β	0.91685	0.52809	0.31685	0.10192	0.31924	0.14512	97.1
	250	θ	1.41333	0.00952	0.01333	0.01000	0.10002	0.38305	96.9
		β	0.91627	0.52712	0.31627	0.10117	0.31808	0.13277	97.2
	300	θ	1.41293	0.00923	0.01293	0.00775	0.08802	0.34123	97.4
		β	0.91551	0.52586	0.31551	0.10032	0.31673	0.12467	96.7
	350	θ	1.41199	0.00857	0.01199	0.00674	0.08211	0.31520	96.7
		β	0.91513	0.52522	0.31513	0.10023	0.31659	0.11346	97.1
	400	θ	1.41139	0.00813	0.01139	0.00601	0.07754	0.30081	97.2
		β	0.91465	0.52441	0.31465	0.09980	0.31592	0.11088	97.0
	450	θ	1.40637	0.00455	0.00637	0.00475	0.06892	0.26913	97.1
		β	0.91365	0.52275	0.31365	0.09922	0.31498	0.10218	96.8

Table 4
Parameter estimates and goodness-of-fit measures of the kidney dialysis patient dataset

Distribution	Estimates (S.E)	*LogL*	*AIC*	*BIC*	*CAIC*	*HQIC*	*KS*	*p-value*
BTILBE(θ, β)	$\hat{\beta} = 1.01$ (3.4527) $\hat{\theta} = 0.4750$ (9.1717)	2.7897	-1.5794	1.0849	-1.0994	-0.7648	0.1135	0.8634
KMILBE(θ)	$\hat{\theta} = 0.562$ (0.069)	2.205	-2.411	-2.964	-2.257	-2.003	0.1375	0.665
SIR(θ)	$\hat{\theta} = 0.237$ (0.017)	10.921	23.842	23.289	23.996	24.249	0.3061	0.0105
IE(θ)	$\hat{\theta} = 0.237$ (0.045)	1.248	4.496	3.943	4.958	4.903	0.2279	0.1091
IL(θ)	$\hat{\theta} = 3.270$ (0.520)	0.294	2.588	2.742	2.742	2.996	0.1554	0.5084

- Set 2 = (θ = 2.1 and β = 1.1)
- Set 3 = (θ = 1.8 and β = 0.8)
- Set 4 = (θ = 0.8 and β = 0.5)
- Set 5 = (θ = 1.5 and β = 0.2)
- Set 6 = (θ = 0.7 and β = 1.3)
- Set 7 = (θ = 1.1 and β = 0.9)
- Set 8 = (θ = 2.5 and β = 0.5)
- Set 9 = (θ = 2.2 and β = 1.1)
- Set 10 = (θ = 1.4 and β = 0.6)

The parameter estimates for these sets are presented in Table 3. The results presented in Table 3 show that MSE, RBias, bias, RMSE, and AIL all decrease significantly with an increasing sample size (n).

8. Real Data Application

In this section, we evaluate the performance of the newly introduced BTILBE distribution by analyzing two real-world datasets. We

Table 5
Parameter estimates and goodness-of-fit measures of stream flow amounts at USGS station 9-3425

Distribution	Estimates	*LogL*	*AIC*	*BIC*	*CAIC*	*HQIC*	*KS*	*p-value*
BTILBE(θ, β)	$\hat{\beta} = 137.0563$ (217.6824) $\hat{\theta} = 665.3262$ (85.0192)	207.0158	418.0316	421.1423	418.4066	419.1054	0.1247	0.608
ILBE(θ)	$\hat{\theta} = 360.4776$ (43.0854)	213.3170	428.6341	430.1894	428.7552	429.1709	0.1986	0.1098
SIE(θ)	$\hat{\theta} = 235.3634$ (30.5340)	214.7691	431.5381	433.0934	431.6594	432.0751	0.2049	0.0912
SIR(θ)	$\hat{\theta} = 30,784.82$ (3751.5)	232.5056	467.0125	468.5678	467.1324	467.5481	0.2105	0.0771
IE(θ)	$\hat{\theta} = 180.2399$ (30.4660)	223.4931	448.9863	450.5416	449.1074	449.5231	0.3335	< 0.005
IL(θ)	$\hat{\theta} = 180.8855$ (30.4089)	223.4928	448.9855	450.5409	449.1068	449.5225	0.3329	< 0.005
KMILBE(θ)	$\hat{\theta} = 256.2931$ (38.9452)	416.0894	834.1788	835.7341	834.3	834.7157	0.40067	< 0.005

Figure 4
The TTT plot, box plot, and violin plot for the kidney dialysis patient data

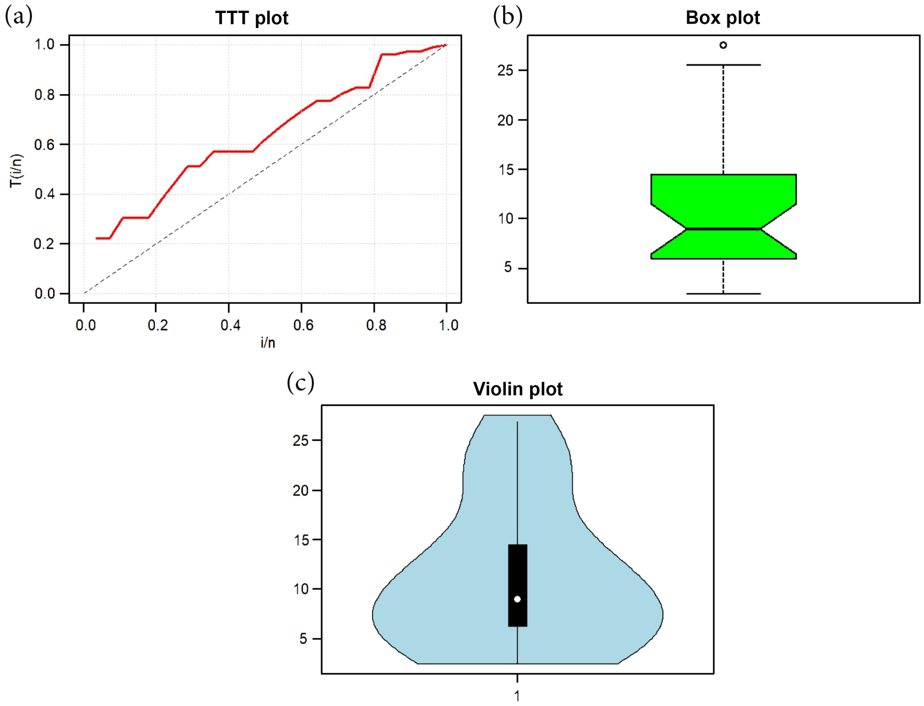

compare the performance of the BTILBE distribution with several other continuous distributions, as listed in Tables 4 and 5. To assess goodness of fit, we employ a range of statistical measures, including the negative log-likelihood ($Log\ L$), Akaike information criterion (AIC), corrected AIC ($CAIC$), Bayesian information criterion (BIC), Hannan-Quinn information criterion ($HQIC$), Kolmogorov-Smirnov test (KS), and

Figure 5
Fitted distributions and diagnostic plots for the kidney dialysis patient dataset: (a) PDF, (b) CDF, (c) SF, and (d) PP plot

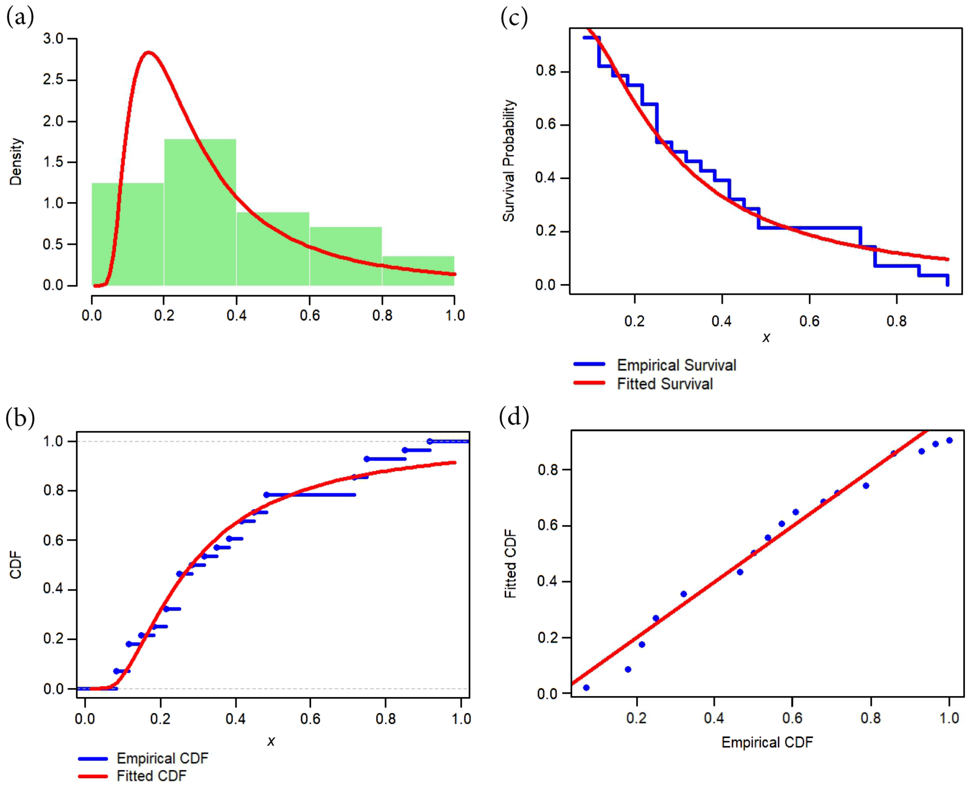

Figure 6
Fitted PDF plots comparing alternative distributions for the kidney dialysis patient dataset

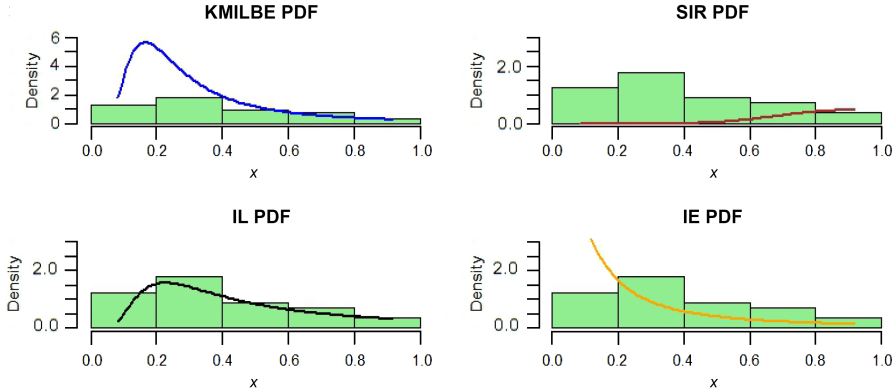

the corresponding $p - value$. These metrics provide a comprehensive evaluation of how well each distribution fits the data.

In this study, we examine two real-world datasets to assess the effectiveness of the newly proposed BTILBE distribution. The first dataset consists of the times to infection (in months) for kidney dialysis patients, as studied by Klein and Moeschberger [45].

Figure 4 illustrates the total time on test (TTT) plot, box plot, and violin plot for the kidney dialysis patient dataset. The TTT plot exhibits a convex shape, indicating an increasing failure rate over time. The box plot reveals a moderately right-skewed distribution, with the median positioned closer to the lower quartile and a longer upper whisker compared to the lower one. This suggests the presence of a few larger values that stretch the distribution to the right. The violin plot supports this observation, showing a higher density of values at the lower end and a longer tail extending to the right, confirming positive skewness in the data.

Maximum likelihood estimates (MLEs) for various competing continuous models, along with their standard errors (SEs) and goodness-of-fit evaluations, are systematically presented in Table 4 for the kidney dialysis patient datasets. To facilitate visual comparison, plots of the fitted CDFs, PDFs, SFs, and probability-probability (PP) plots for the fitted distributions are included in Figure 5. Additionally, Figures 6 and 7 show the fitted PDFs and CDFs of the competing alternative distributions for these datasets.

The findings presented in Table 4 demonstrate that the BTILBE model outperforms other competing distributions. It consistently achieves the lowest values across all statistical metrics, including the Kolmogorov-Smirnov (KS) distance, indicating a better fit to the data. This highlights the effectiveness of the BTILBE distribution in accurately modeling real-world datasets.

Figure 8 presents the likelihood functions of the unimodal profile and a contour graph for the BTILBE parameters of the dataset of kidney dialysis patients. Subplot (a) displays the log-likelihood as a function of parameter β, showing a clear peak with a steep decline, indicating a well-defined maximum likelihood estimate. Subplot (a) illustrates the log-likelihood as a function of parameter θ, also exhibiting a distinct peak, suggesting a unimodal distribution. Contour plot (b) visualizes the joint log-likelihood across β and θ, with a red dot marking the maximum likelihood estimate. The color gradient, ranging from yellow to purple, highlights the varying likelihood values, with the peak centered around the optimal parameter combination.

The second dataset comprises stream flow amounts (measured in 1,000 feet) recorded over a 35-year period (1936–1970) at US Geological Survey (USGS) gauging station number 9-3425. This dataset, originally studied by Mielke and Johnson [46], includes annual stream flow measurements taken from April 1 to August 31 for each year. Figure 9 displays the TTT plot, box plot, and violin plot for

Figure 7
Fitted CDF plots comparing alternative distributions for the kidney dialysis patient dataset

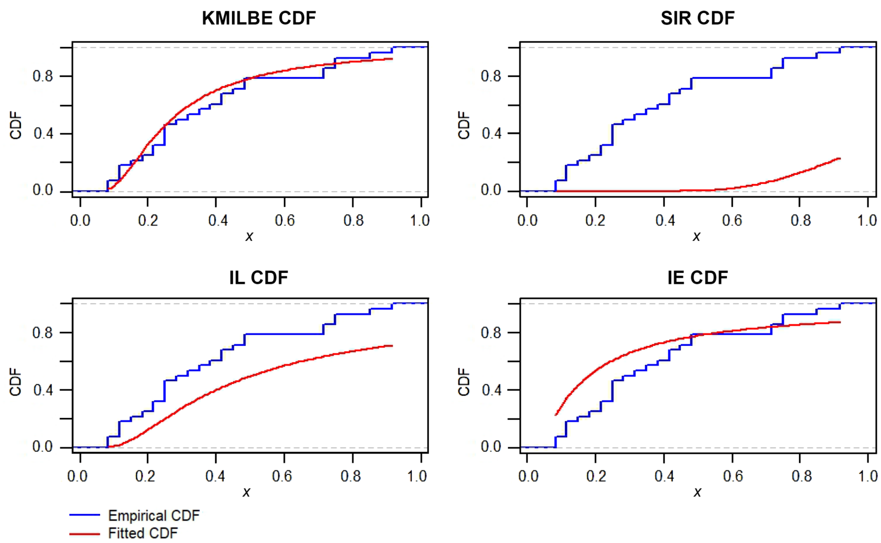

Figure 8
Unimodal profile likelihood functions and contour plot of BTILBE distribution parameters for the kidney dialysis patient dataset

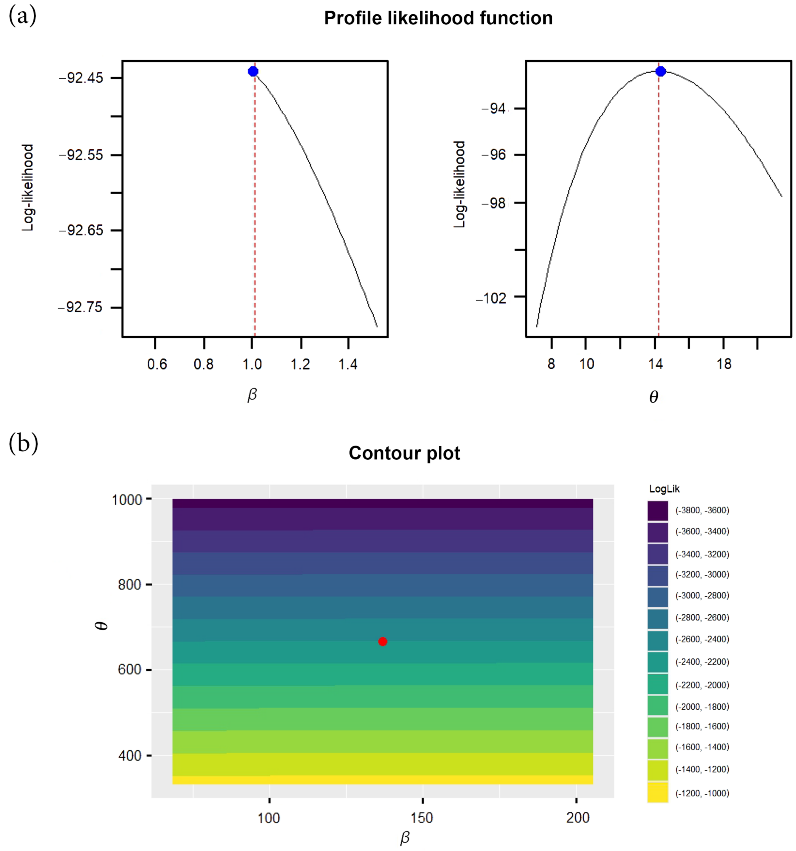

Figure 9
The TTT plot, box plot, and violin plot for the stream flow amounts at USGS station 9-3425

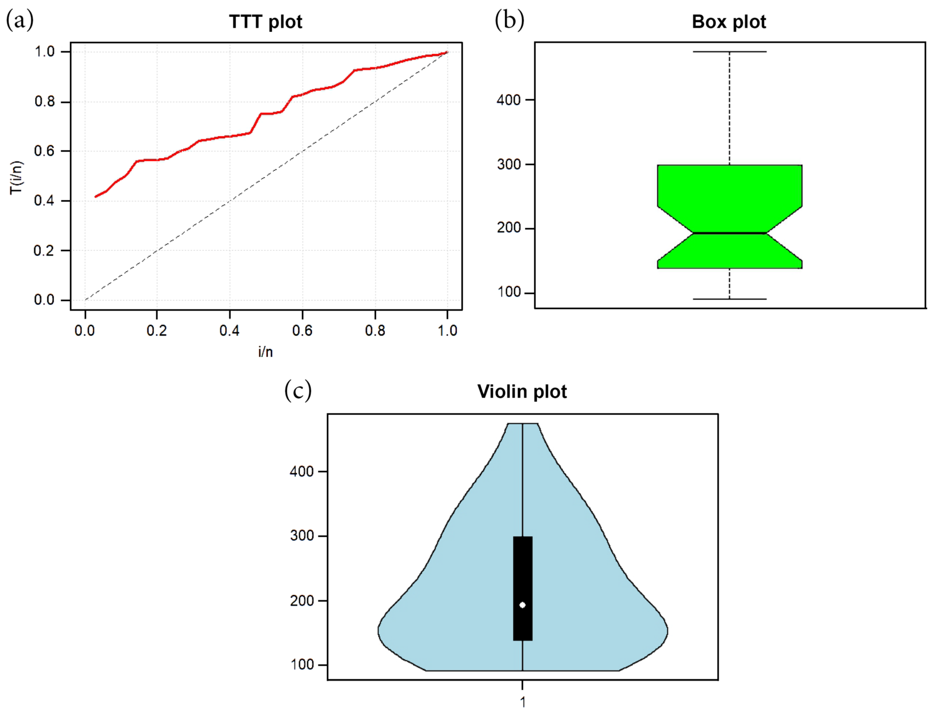

Figure 10
Unimodal profile likelihood function and contour plot of BTILBE distribution parameters for stream flow amounts at USGS station 9-3425

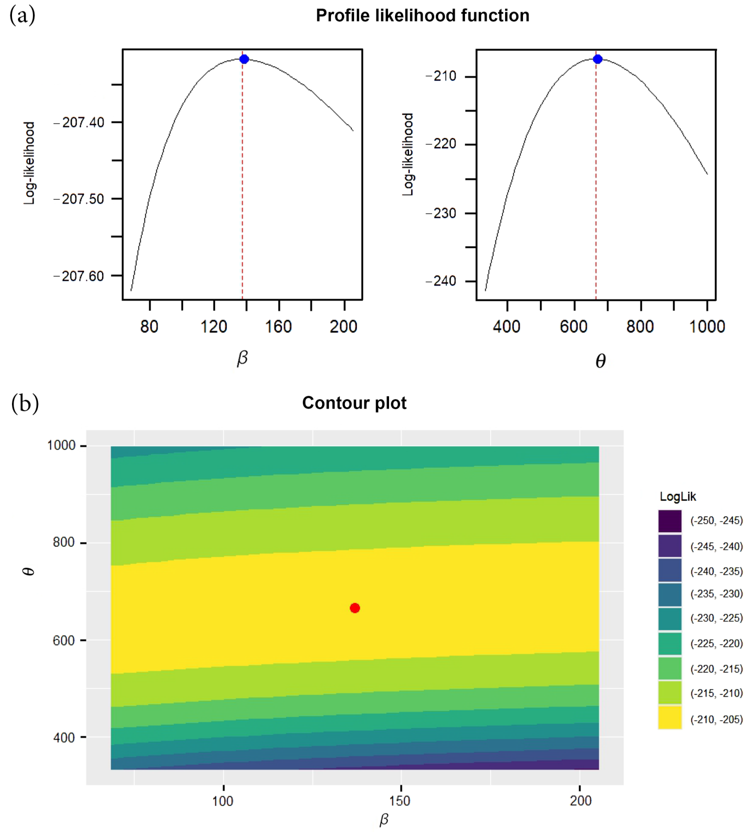

Figure 11
Fitted distributions and diagnostic plots for stream flow amounts at USGS station 9-3425: (a) PDF, (b) CDF, (c) SF, and (d) PP plot

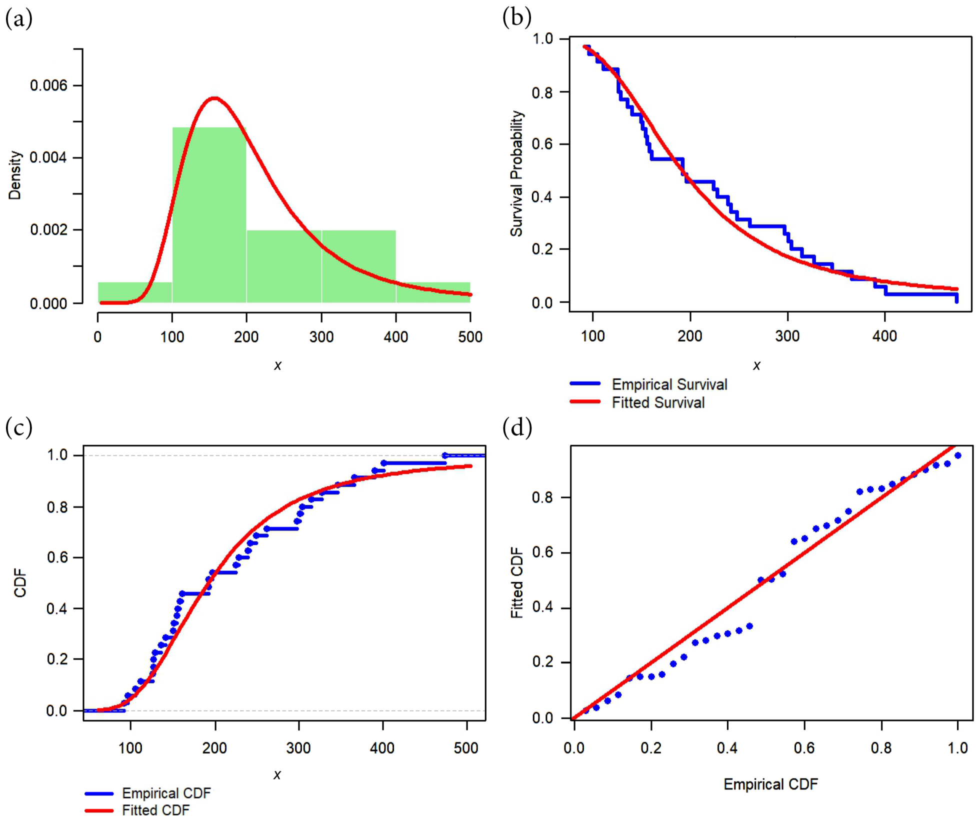

Figure 12
Fitted PDF plots comparing alternative distributions for the annual stream flow measurements at USGS station 9-3425

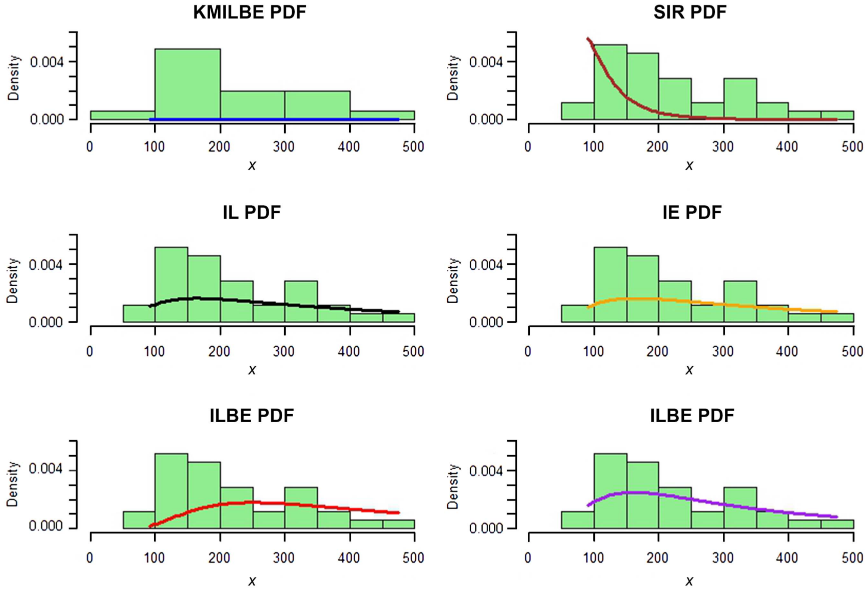

the stream flow amounts dataset. The TTT plot shows a convex trend, suggesting an increasing failure rate with varying behavior. The box plot indicates a strongly right-skewed distribution, as the median lies closer to the lower quartile, the upper whisker is significantly longer than the lower one, and several higher values extend the upper range. The violin plot reinforces this finding, highlighting a dense concentration of values at the lower end and a pronounced rightward tail, confirming the positive skewness of the data distribution.

Figure 10 presents the likelihood functions with a unimodal profile and a contour plot for the BTILBE parameters of the stream flow amounts dataset. Subplot (a) displays the log-likelihood as a function of parameter β, exhibiting a distinct peak, confirming a unimodal profile. The contour plot in Figure 10(b) shows the joint log-likelihood surface for the parameters β and θ, with a red dot marking the maximum likelihood estimate. The color gradient ranges from yellow (higher log-likelihood values) to purple (lower values), clearly indicating that the peak occurs at the optimal parameter combination.

The maximum likelihood estimates (MLEs) for various competing continuous models, along with their standard errors (SEs) and goodness-of-fit metrics, are systematically presented in Table 5. An analysis of this table reveals that the BTILBE distribution exhibits the lowest values for AIC, BIC, CAIC, HQIC, and KS statistics, along with the highest p-value. This indicates that the BTILBE distribution provides a superior fit compared to the other competing models. These

Figure 13
Fitted CDF plots comparing alternative distributions for the annual stream flow measurements at USGS station 9-3425

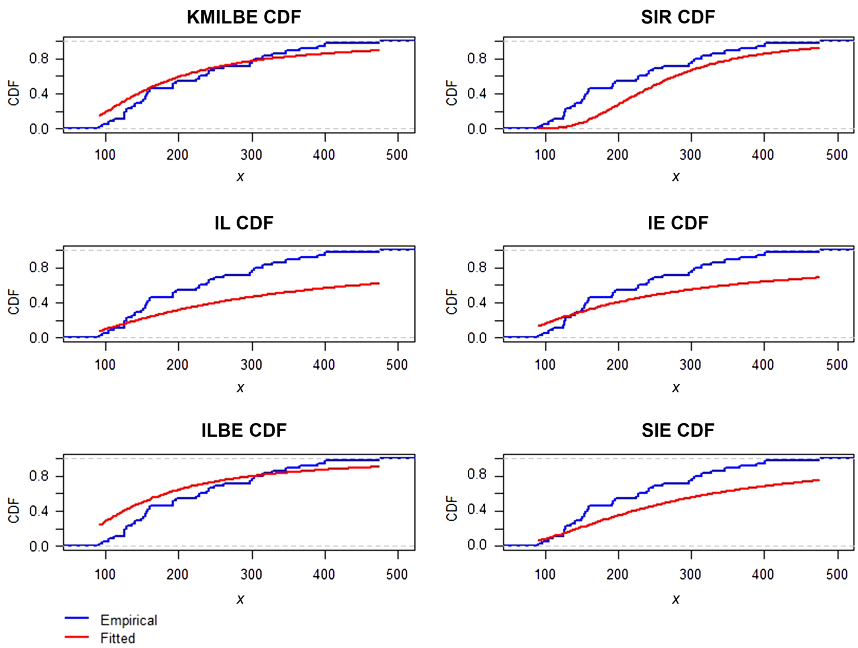

findings are visually supported in Figure 5, which includes the fitted density plot, CDF, SF, and P-P plot. The plots of the fitted PDFs and CDFs for the competing alternative distributions are presented in Figures 11, 12, and 13.

9. Conclusion

This paper proposes the BTILBE distribution, a novel extension of the ILBE distribution. Its PDF exhibits decreasing, unimodal, and right-skewed shapes, while the HRF displays decreasing, increasing, or upside-down bathtub patterns, illustrated via 2D and 3D plots. These features suit the BTILBE for modeling diverse failure behaviors. We derive key statistical properties, including moments, incomplete moments, MGF, entropy measures (Shannon, Tsallis, and Rényi), mean residual life, and mean inactivity time, with numerical analysis. Parameters are estimated via MLE, with consistency verified through Monte Carlo simulations. Applications to kidney dialysis patient data and USGS stream flow data demonstrate superior fit over competing models, evidenced by lowest AIC, BIC, HQIC, CAIC, highest KS p-values, and supportive PDF, CDF, SF, and PP plots. Thus, the BTILBE offers a versatile, robust modeling tool. Future work will explore additional properties and Bayesian estimation.

Acknowledgement

The authors would like to express their sincere gratitude to the reviewers for their valuable and constructive comments that have greatly improved the quality of this work. This research was supported by Imam Mohammad Ibn Saud Islamic University (IMSIU). The first author gratefully acknowledges IMSIU for its technical and financial support.

Funding Statement

This work was supported and funded by the Deanship of Scientific Research at Imam Mohammad Ibn Saud Islamic University (IMSIU) (grant number IMSIU-DDRSP-RP25).

Ethical Statement

This study does not contain any studies with human or animal subjects performed by any of the authors.

Conflicts of Interest

The authors declare that they have no conflicts of interest to this work.

Data Availability Statement

The data supporting the findings of this study are openly available at https://doi.org/10.1007/0-387-21645-6_3, reference number [45], and https://doi.org/10.1175/1520-0493(1973)101<0701:TKDMLE>2.3.CO;2, reference number [46].

Author Contribution Statement

Jabir Bengalath: Conceptualization, Methodology, Software, Formal analysis, Investigation, Writing – review & editing, Visualization, Supervision. **Mohamed Nejib Ouertani:** Software, Validation, Formal analysis, Data curation. **Hanene Hamdani:** Software, Validation, Formal analysis, Data curation. **Fasna Kottakkunnan:** Conceptualization, Methodology, Software, Resources. **Mohammed Elgarhy:** Validation, Investigation, Writing – original draft, Writing – review & editing, Project administration, Funding acquisition.

References

[1] Hussain, S., Rashid, M. S., Ul Hassan, M., & Ahmed, R. (2022). The generalized exponential extended exponentiated family of distributions: Theory, properties, and applications. *Mathematics*, *10*(19), 3419. https://doi.org/10.3390/math10193419

[2] Hassan, A. S., Mohamed, R. E., Kharazmi, O., & Nagy, H. F. (2022). A new four parameter extended exponential distribution with statistical properties and applications. *Pakistan Journal of Statistics and Operation Research*, *18*(1), 179–193. https://doi.org/10.18187/pjsor.v18i1.3872

[3] Usman, U., Shamsuddeen, S., Arkilla, B. M., & Aliyu, Y. (2020). Inferences on the Weibull exponentiated exponential distribution and applications. *International Journal of Statistical Distributions and Applications*, *6*(1), 10–22. https://doi.org/10.11648/j.ijsd.20200601.12

[4] Radwan, H., Mahmoud, M., & Ghazal, M. (2024). Modified generalized linear exponential distribution: Properties and applications. *Statistics, Optimization & Information Computing*, *12*(1), 231–255. https://doi.org/10.19139/soic-2310-5070-1103

[5] Bengalath, J., & Punathumparambath, B. (2023). A novel extension of inverse exponential distributions: A heavy-tailed model with upside-down bathtub-shaped hazard rate. *Reliability: Theory & Applications*, *18*(4(76)), 112–127. https://doi.org/10.24412/1932-2321-2023-476-112-127

[6] Saboor, A., Jamal, F., Shafq, S., & Mumtaz, R. (2025). On the versatility of the unit logistic exponential distribution: Capturing bathtub, upside-down bathtub, and monotonic hazard rates. *Innovation in Statistics and Probability*, *1*(1), 28–46. https://doi.org/10.64389/isp.2025.01102

[7] Noori, N. A., Khaleel , M. A., Khalaf , S. A., & Dutta, S. (2025). Analytical modeling of expansion for Odd Lomax generalized exponential distribution in framework of neutrosophic logic: A theoretical and applied on neutrosophic data. *Innovation in Statistics and Probability*, *1*(1), 47–59. https://doi.org/10.64389/isp.2025.01104

[8] Orji, G. O., Etaga, H. O., Almetwally, E. M., Igbokwe, C. P., Aguwa, O. C., & Obulezi, O. J.(2025). A new odd reparameterized exponential transformed-X family of distributions with applications to public health data. *Innovation in Statistics and Probability*, *1*(1), 88–118. https://doi.org/10.64389/isp.2025.01107

[9] Elsherpieny, E., & Abdel-Hakim, A. (2025). Statistical analysis of alpha-power exponential distribution using unified hybrid censored data and its applications. *Computational Journal of Mathematical and Statistical Sciences*, *4*(1), 283–315. https://doi.org/10.21608/cjmss.2025.346134.1094

[10] Abdelall, Y. Y. (2024). Statistical properties of a generalization Erlang truncated exponential distribution with applications and its bivariate extension. *Computational Journal of Mathematical and Statistical Sciences*, *3*(2), 258–279. https://doi.org/10.21608/cjmss.2024.277233.1045

[11] Korkmaz, M. Ç., Altun, E., Alizadeh, M., & El-Morshedy, M. (2021). The log exponential-power distribution: Properties, estimations and quantile regression model. *Mathematics*, *9*(21), 2634. https://doi.org/10.3390/math9212634

[12] Eliwa, M. S., El-Morshedy, M., & Yousof, H. M. (2022). A discrete exponential generalized-G family of distributions: Properties with Bayesian and non-Bayesian estimators to model

medical, engineering and agriculture data. *Mathematics*, *10*(18), 3348. https://doi.org/10.3390/math10183348

[13] Abonongo, A., & Abonongo, J. (2024). Exponentiated generalized Weibull exponential distribution: Properties, estimation and applications. *Computational Journal of Mathematical and Statistical Sciences*, *3*(1), 57–84. https://doi.org/10.21608/cjmss.2023.243845.1023

[14] Mushtaq, A., Hussain, T., Shakil, M., Ahsanullah, M., & Kibria, B. M. G. (2025). Exponentiated inverse exponential distribution: Properties and applications. *Axioms*, *14*(10), 753. https://doi.org/10.3390/axioms14100753

[15] Aljohani, H. M., Almetwally, E. M., Alghamdi, A. S., & Hafez, E. H. (2021). Ranked set sampling with application of modified Kies exponential distribution. *Alexandria Engineering Journal*, *60*(4), 4041–4046. https://doi.org/10.1016/j.aej.2021.02.043

[16] Jamal, F., Chesneau, C., & Elgarhy, M. (2020). Type II general inverse exponential family of distributions. *Journal of Statistics and Management Systems*, *23*(3), 617–641. https://doi.org/10.1080/09720510.2019.1668159

[17] Alghamdi, S. M., Shrahili, M., Hassan, A. S., Gemeay, A. M., Elbatal, I., & Elgarhy, M. (2023). Statistical inference of the half logistic modified Kies exponential model with modeling to engineering data. *Symmetry*, *15*(3), 586. https://doi.org/10.3390/sym15030586

[18] Sapkota, L. P., Bam, N., & Kumar, V. (2025). A new exponential family of distributions with applications to engineering and medical data. *Scientific Reports*, *15*(1), 33649. https://doi.org/10.1038/s41598-025-14890-4

[19] Alkhazaleh, M., Alkhazaleh, S., Handam, A., Abu-Saleem, A., & Alkhazaleh, A. M. H. (2024). Extended exponential distribution with application on financial data. *Applied Mathematics & Information Sciences*, *18*(6), 1455–1467. https://doi.org/10.18576/amis/180622

[20] Noori, N. A., Khaleel, M. A., & Salih, A. M. (2025). Some expansions to the Weibull distribution families with two parameters: A review. *Babylonian Journal of Mathematics*, *2025*, 61–87. https://doi.org/10.58496/BJM/2025/008

[21] Hussain, A. S., Jameel, A. F., Az-Zo'Bi, E. A., & Tashtoush, M. A. (2025). Enhanced parameter estimation for the modified Gompertz-Makeham model in nonhomogeneous Poisson processes using modified likelihood and swarm intelligence approaches. *Babylonian Journal of Mathematics*, *2025*, 32–43. https://doi.org/10.58496/BJM/2025/005

[22] Dara, S. T., & Ahmad, M. (2012). *Recent advances in moment distributions and their hazard rate*. Germany: Lap Lambert Academic Publishing.

[23] Fisher, R. A. (1934). The effects of methods of ascertainment upon the estimation of frequencies. *Annals of Eugenics*, *6*(1), 13–25. https://doi.org/10.1111/j.1469-1809.1934.tb02105.x

[24] Rao, C. R. (1965). On discrete distributions arising out of methods of ascertainment. *Sankhyā: The Indian Journal of Statistics*, *27*(2–4), 311–324.

[25] Ahsan ul Haq, M., Usman, R. M., Hashmi, S., & Al-Omeri, A. I. (2019). The Marshall-Olkin length-biased exponential distribution and its applications. *Journal of King Saud University - Science*, *31*(2), 246–251. https://doi.org/10.1016/j.jksus.2017.09.006

[26] Mathew, J. (2020). Harris extended length-biased exponential distribution and its applications. *International Journal of Mathematics and Computational Research*, *8*(4), 2035–2041. https://doi.org/10.33826/ijmcr/v8i4.01

[27] Abdelwahab, M. M., Elbatal, I., Elgarhy, M., Ghorbal, A. B., Semary, H. E., & Almetwally, E. M. (2024). A new extension of inverse length biased exponential model with statistical inference under joint censored samples and application. *Alexandria Engineering Journal*, *99*, 377–393. https://doi.org/10.1016/j.aej.2024.04.068

[28] Kumar, S., & HaraGopal, V. V. (2021). Higher order moments of the order statistics for the rectangular, exponential, gamma and Weibull distributions. *European Journal of Mathematics and Statistics*, *2*(3), 61–76. https://doi.org/10.24018/ejmath.2021.2.3.23

[29] Wen, X. (2022). Numerical characteristic analysis of order statistics under exponential distribution. *Academic Journal of Mathematical Sciences*, *3*(2), 22–28. https://doi.org/10.25236/AJMS.2022.030204

[30] AL-Zaydi, A. M. (2023). Log-extended exponential–geometric distribution: Moments and inference based on generalized order statistics. *Symmetry*, *15*(10), 1857. https://doi.org/10.3390/sym15101857

[31] Sobhi, A. L., & Mashail, M. (2022). Moments of dual generalized order statistics and characterization for transmuted exponential model. *Computational Journal of Mathematical and Statistical Sciences*, *1*(1), 42–50. 10.21608/cjmss.2022.272548

[32] Akhter, Z., MirMostafaee, S. M. T. K., & Ormoz, E. (2022). On the order statistics of exponentiated moment exponential distribution and associated inference. *Journal of Statistical Computation and Simulation*, *92*(6), 1322–1346. https://doi.org/10.1080/00949655.2021.1991927

[33] Almuhayfith, F. E., Alam, M., Bakouch, H. S., Bapat, S. R., & Albalawi, O. (2024). Linear combination of order statistics moments from log-extended exponential geometric distribution with applications to entropy. *Mathematics*, *12*(11), 1744. https://doi.org/10.3390/math12111744

[34] Balakrishnan, N., & Bhattacharya, R. (2022). Revisiting best linear unbiased estimation of location-scale parameters based on optimally selected order statistics using compound design. *Methodology and Computing in Applied Probability*, *24*(3), 1891–1915. https://doi.org/10.1007/s11009-021-09891-5

[35] Gupta, R. C., Gupta, P. L., & Gupta, R. D. (1998). Modeling failure time data by Lehman alternatives. *Communications in Statistics - Theory and Methods*, *27*(4), 887–904. https://doi.org/10.1080/03610929808832134

[36] Shaw, W. T., & Buckley, I. R. C. (2009). *The alchemy of probability distributions: Beyond Gram-Charlier expansions, and a skew-kurtotic-normal distribution from a rank transmutation map*. arXiv. https://doi.org/10.48550/arXiv.0901.0434

[37] Kumar, D., Singh, U., & Singh, S. K. (2015). A method of proposing new distribution and its application to bladder cancer patients data. *Journal of Statistical Applications and Probability Letters*, *2*(3), 235–245. http://dx.doi.org/10.12785/jsapl/020306

[38] Maurya, S. K., Kaushik, A., Singh, S. K., & Singh, U. (2017). A new class of distribution having decreasing, increasing, and bathtub-shaped failure rate. *Communications in Statistics - Theory and Methods*, *46*(20), 10359–10372. https://doi.org/10.1080/03610926.2016.1235196

[39] Kumar, D., Kumar, P., Kumar, P., Singh, S. K., & Singh, U. (2021). PCM transformation: Properties and their estimation. *Journal of Reliability and Statistical Studies*, *14*(2), 373–392. https://doi.org/10.13052/jrss0974-8024.1421

[40] Mahdavi, A., & Kundu, D. (2017). A new method for generating distributions with an application to exponential distribution. *Communications in Statistics - Theory and Methods*, *46*(13), 6543–6557. https://doi.org/10.1080/03610926.2015.1130839

[41] Lone, M. A., & Jan, T. R. (2023). A new Pi-exponentiated method for constructing distributions with an application to Weibull distribution. *Reliability: Theory and Applications*, *18*(1(72)), 94–109. https://doi.org/10.24412/1932-2321-2023-172-94-109

[42] Dileepkumar, M., & Bengalath, J. (2025). A new distorted transformation with applications to reliability analysis. *Journal of Statistical Computation and Simulation*, *95*(17), 3776–3798. https://doi.org/10.1080/00949655.2025.2544193

[43] Fasna, K. (2022). A method for generating lifetime models and its application to real data. *Reliability: Theory and Applications*, *17*(4(71)), 344–357. https://doi.org/10.24412/1932-2321-2022-471-344-357

[44] Fasna, K. (2025). A method for generating distributions with an application to Cauchy distribution. *Research in Statistics*, *3*(1), 2462301. https://doi.org/10.1080/27684520.2025.2462301

[45] Klein, J. P., & Moeschberger, M. L. (2006). Censoring and truncation. In J. P. Klein & M. L. Moeschberger (Eds.), *Survival analysis: Techniques for censored and truncated data* (pp. 63—90). Springer. https://doi.org/10.1007/0-387-21645-6_3

[46] Mielke, P. W., & Johnson, E. S. (1973). Three parameter kappa distribution maximum likelihood estimations and likelihood ratio tests. *Monthly Weather Review*, *101*(9), 701–707. https://doi.org/10.1175/1520-0493(1973)101⟨0701:TKDMLE⟩2.3.CO;2

How to Cite: Bengalath, J., Ouertani, M. N., Hamdani, H., Kottakkunnan, F., & Elgarhy, M. (2025). Beta-Transformed Inverse Length-Biased Exponential Distribution: Properties and Applications. *Journal of Computational and Cognitive Engineering*. https://doi.org/10.47852/bonviewJCCE52027030

Appendix

Derivation of the r-th Moment

The r-th moment of a random variable X following the BTILBE distribution is:

$$\mu'_r = E(X^r) = \int_0^\infty x^r g(x)\, dx.$$

Substituting the BTILBE density function:

$$\mu'_r = \frac{\beta \log \beta}{\beta - 1} \theta^2 \int_0^\infty x^{r-3} e^{-\frac{\theta}{x}} \beta^{-(1+\frac{\theta}{x})e^{-\frac{\theta}{x}}}\, dx.$$

Using the series expansion:

$$\beta^{-(1+\frac{\theta}{x})e^{-\frac{\theta}{x}}} = \sum_{k=0}^{\infty} \frac{(-\log \beta)^k}{k!} \left(1 + \frac{\theta}{x}\right)^k e^{-k\frac{\theta}{x}}, \qquad (25)$$

and binomial expansion $\left(1 + \frac{\theta}{x}\right)^k = \sum_{m=0}^{k} \binom{k}{m} \frac{\theta^m}{x^m}$, we get:

$$\mu'_r = \frac{\beta \log \beta}{\beta - 1} \theta^2 \sum_{k=0}^{\infty} \frac{(-\log \beta)^k}{k!} \sum_{m=0}^{k} \binom{k}{m} \theta^m \int_0^\infty x^{r-3-m} e^{-\frac{\theta}{x}(1+k)}\, dx.$$

With substitution $y = \frac{\theta(1+k)}{x}$, $dx = -\frac{\theta(1+k)}{y^2}\, dy$, the integral is:

$$\int_0^\infty x^{r-3-m} e^{-\frac{\theta}{x}(1+k)}\, dx = \theta^{r-2-m}(1+k)^{r-2-m}\Gamma[m+2-r].$$

Thus, we get the r-th moment.

Derivation of the r-th Inverted Moment

The r-th inverted moment is:

$$\mu^*_r = E\left(\frac{1}{x^r}\right) = \int_0^\infty x^{-r} f(x)\, dx.$$

Substituting the BTILBE density function:

$$\mu^*_r = \frac{\beta \log \beta}{\beta - 1} \theta^2 \int_0^\infty x^{-r} e^{-\frac{\theta}{x}} \beta^{-(1+\frac{\theta}{x})e^{-\frac{\theta}{x}}}\, dx.$$

Using Equation (25) and the binomial expansion, we obtain:

$$\mu^*_r = \frac{\beta \log \beta}{\beta - 1} \theta^2 \sum_{k=0}^{\infty} \frac{(-\log \beta)^k}{k!} \sum_{m=0}^{k} \binom{k}{m} \theta^m \int_0^\infty x^{-r+m} e^{-\frac{\theta}{x}(1+k)}\, dx.$$

With substitution $y = \frac{\theta(1+k)}{x}$, the integral is:

$$\int_0^\infty x^{-r+m} e^{-\frac{\theta}{x}(1+k)}\, dx = \theta^{m-r+2}(1+k)^{m-r+2}\Gamma[r-m-2].$$

Thus, we get the r-th inverted moment.

Derivation of the r-th Incomplete Moment

The r-th incomplete moment is:

$$\mu'_r(t) = E(X^r; X \le t) = \int_0^t x^r g(x)\, dx.$$

Substituting the BTILBE density function:

$$\mu'_r(t) = \frac{\beta \log \beta}{\beta - 1} \theta^2 \int_0^t x^{r-3} e^{-\frac{\theta}{x}} \beta^{-(1+\frac{\theta}{x})e^{-\frac{\theta}{x}}}\, dx.$$

Using Equation (25) and the binomial expansion:

$$\mu'_r(t) = \frac{\beta \log \beta}{\beta - 1} \theta^2 \sum_{k=0}^{\infty} \frac{(-\log \beta)^k}{k!} \sum_{m=0}^{k} \binom{k}{m} \theta^m \int_0^t x^{r-3-m} e^{-\frac{\theta}{x}(1+k)}\, dx.$$

With substitution $y = \frac{\theta(1+k)}{x}$, the integral is:

$$\int_0^t x^{r-3-m} e^{-\frac{\theta}{x}(1+k)}\, dx = \theta^{r-2-m}(1+k)^{r-2-m}\Gamma_u(m+2-r, \frac{\theta(1+k)}{t}),$$

where $\Gamma_u(s, a) = \int_a^\infty y^{s-1} e^{-y}\, dy$. Thus, we get the r-th incomplete moment.